

Design of an Optimal Super Twisting Sliding Mode Controller for the
Application of Voltage Control of a DC-DC Buck-Boost Converter



Hailegebriel Adera Lemma

A Thesis Submitted to the Department of Electrical Power and Control
Engineering
School of Electrical Engineering and Computing

Presented in Partial Fulfillment of the Requirement for the Degree of
Master's in Electrical Power and Control Engineering (Control Engineering)

Office of Graduate Studies
Adama Science and Technology University

July 2023
Adama, Ethiopia

Design of an Optimal Super Twisting Sliding Mode Controller for the
Application of Voltage Control of a DC-DC Buck-Boost Converter

Hailegebriel Adera Lemma

Advisor: Dr. Shubhashish Bhakta (Ph.D. Engg.)

A Thesis Submitted to the Department of Electrical Power and Control
Engineering

School of Electrical Engineering and Computing

Presented in Partial Fulfillment of the Requirement for the Degree of
Master's in Electrical Power and Control Engineering (Control Engineering)

Office of Graduate Studies

Adama Science and Technology University

July 2023
Adama, Ethiopia

DECLARATION

I hereby declare that this Master Thesis entitled “Design of an Optimal Super Twisting Sliding Mode Controller for the Application of Voltage Control of a DC-DC Buck-Boost Converter” is my original work. That is, it hasn’t been submitted for the award of any academic diploma, degree, or certificate in any other university. All sources of materials that are used for this thesis have been duly acknowledged through citation.

Hailegebriel Adera Lemma

Name of student

Signature

Date

RECOMMENDATION

I, the advisor of this thesis, hereby certify that I have read the revised version of the thesis entitled “Design of an Optimal Super Twisting Sliding Mode Controller for the Application of Voltage Control of a DC-DC Buck-Boost Converter” prepared under my guidance by Hailegebriel Adera submitted in partial fulfilment of the requirement for the degree of Master of Science in Electrical Power and Control Engineering, postgraduate in Control Engineering.

Therefore, I recommend the submission of revised version of the thesis to the department following the applicable procedures.

Dr. Shubhashish Bhakta

Name of Advisor

Signature

Date

APPROVAL SHEET

I, the advisor of the thesis entitled “Design of an Optimal Super Twisting Sliding Mode Controller for the Application of Voltage Control of a DC-DC Buck-Boost Converter” and developed by Hailegebriel Adera, hereby certify that the recommendation and suggestions made by the board of examiners are appropriately incorporated into the final version of the thesis.

Dr. Shubhashish Bhakta

Advisor

Signature

Date

We, the undersigned, members of the Board of Examiners of the thesis by Hailegebriel Adera have read and evaluated the thesis entitled “Design of an Optimal Super Twisting Sliding Mode Controller for the Application of Voltage Control of a DC-DC Buck-Boost Converter” and examined the candidate during open defence. This is to certify that the thesis has been accepted in partial fulfilment of the requirement of the Degree of Master’s in control engineering.

Chairperson

Signature

Date

Internal Examiner

Signature

Date

External Examiner

Signature

Date

Finally, approval and acceptance of the thesis is contingent upon submission of its final copy to the Office of Postgraduate Studies (OPGS) through the Department Graduate Council (DGC) and School Graduate Committee (SGC).

Department Head

Signature

Date

School Dean

Signature

Date

Office of Postgraduate Studies, Dean

Signature

Date

ACKNOWLEDGMENT

I want to start by thanking God for granting me the opportunity to finish this thesis. My deepest thanks go out to Dr Shubhashish Bhakta, who served as my thesis advisor and who sacrificed a lot of his time to support me, work with me, and offer me the freedom to go thoroughly into my topic. I am appreciative of everyone who helped me during my employment by encouraging me and providing me with important support.

TABLE OF CONTENTS

DECLARATION	i
RECOMMENDATION	ii
APPROVAL SHEET	iii
ACKNOWLEDGMENT	iv
TABLE OF CONTENTS.....	v
LIST OF TABLES	viii
LIST OF FIGURES	ix
LIST OF ACRONYMS	xi
LIST OF SYMBOLS.....	xii
ABSTRACT	xiv
CHAPTER ONE.....	1
INTRODUCTION	1
1.1 Background of the study	1
1.2 Statement of the Problem.....	2
1.3 Objectives of the Study	3
1.3.1 General Objectives	3
1.3.2 Specific Objectives.....	3
1.4 Scope of the Study	3
1.5 Limitations of the Study	4
1.6 Significance of the Study	4
1.7 Thesis Organization	4
CHAPTER TWO	5
LITERATURE REVIEW	5
2.1 Related Work	5
2.2 Summary of Literature	8
2.3 System Overview	9
2.3.1 DC-DC Buck-Boost Converter	9
2.3.2 Mode of Operation of Buck-Boost Converter.....	12

2.3.3 Continuous Conduction Mode	13
2.3.4 Discontinuous Conduction Mode.....	13
2.3.5 Functions of Various Buck-Boost Converter Components.....	14
CHAPTER THREE	16
MATERIALS AND METHODS	16
3.1 Chapter Overview	16
3.2 Materials used	16
3.3 Methods	16
3.4 Block diagram of the research work	17
3.5 Analysis of Buck-Boost Converter	18
3.5.1 Calculation of duty ratio.....	18
3.5.2 Converter Analysis when the Switch Closed	18
3.5.3 Converter Analysis for the Switch Open.....	19
3.5.4 Inductor Calculation.....	21
3.5.5 Capacitor Calculation.....	23
3.6 Mathematical Modelling of the system	24
3.7 State-Space Average Model of the System.....	29
3.8 Impact of Parasitic Components on the System Performance	32
3.9 Stability Analysis	33
3.9.1 Equilibrium Points.....	33
3.9.2 Checking stability of non-linear system.....	34
3.9.3 Local stability analysis	34
3.10 System Controller Design.....	35
3.10.1 Sliding mode control	35
3.10.2 Design of super twisting sliding mode controller	37
3.10.3 PID controller for the System	41
3.10.4 The Proposed Methods of Optimization	42
3.10.5 Genetic Algorithms (GA).....	42
3.10.6 Particle Swarm Optimization	43
3.10.7 Objective Functions.....	44
3.10.8 GA based PID controller	44
3.11 Overall System Structure	47
CHAPTER FOUR	50
RESULT AND DISCUSSION	50

4.1 Introduction.....	50
4.2 Simulation result.....	50
4.2.1 System Open Loop Performance.....	51
4.2.2 System Performance with GA-PID.....	53
4.2.3 System Performance with a GA-PID Controller in the Presence of Load Resistance and Input Voltage Disturbance.....	53
4.2.4 System Performance with STSMC.....	55
4.2.5 System Performance with STSMC using staircase reference.....	56
4.2.6 System Performance with STSMC Controller in presence of Disturbance in Load Resistance and Input Voltage.....	56
4.2.7 System Performance Comparison for GA-PID, GA-STSMC and PSO-STSMC.....	58
4.2.8 System Performance Comparison of GA-PID, GA-STSMC and PSO-STSMC with staircase reference.....	59
5 CONCLUSION AND RECOMMENDATION.....	61
5.1 Conclusion.....	61
5.2 Recommendation.....	62
REFERENCES.....	64
APPENDIXES.....	69
Appendix A: Specifications of the system Parameters.....	69
Appendix B: Proposed STSMC Controller in Simulink.....	70
Appendix C: System Simulink Model.....	71
Appendix D: GA Code for Proposed STSMC.....	72
Appendix E: PSO Code for Proposed STSMC.....	73

LIST OF TABLES

Table 3:1 Boundaries for tuning parameters of controller.....	47
Table 3:2 Parameters for the algorithms.....	49
Table 3:3 The proposed STSMC's Optimal values.	49
Table 4:1 System parameters for running the simulation	51
Table 4:2 Comparisons of system performance measures.....	60

LIST OF FIGURES

Figure 2.1 BBC's circuit (Guldemir, 2011a)	11
Figure 2.2 The waveform of BBC during CCM (Guldemir, 2011a)	12
Figure 2.3 The waveform of inductor current during CCM (padhyay et al., 2015)	13
Figure 2.4 The waveform of inductor current during DCM (padhyay et al., 2015)	14
Figure 3.1 Block diagram of the research methodology	17
Figure 3.2 Block diagram of the research work	18
Figure 3.3 Circuit for the converter as the switch is closed	18
Figure 3.4 Circuit for the converter as the switch is open	19
Figure 3.5 BBC circuit diagram	25
Figure 3.6 BBC equivalent circuit	26
Figure 3.7 BBC as the switch is closed	26
Figure 3.8 BBC as the switch is open	28
Figure 3.9 BBC circuit with impact of parasitic elements	32
Figure 3.10 MOSFET with its equivalent circuit	32
Figure 3.11 Phase portrait of sliding motion in SMC	36
Figure 3.12 Trajectory of super-twisting controller	37
Figure 3.13 Block Diagram of PID Controller (Hussein et al., 2015)	41
Figure 3.14 The PID controller for DC-DC Buck-Boost converter	42
Figure 3.15 Structure of the GA-PID Controller	45
Figure 3.16 The convergence characteristic curve.	46
Figure 3.17 Overall system structure	47
Figure 3.18 Convergent curve for GA	48
Figure 3.19 Convergent curve for PSO	48
Figure 4.1 MATLAB/Simulink model of the proposed system	50
Figure 4.2 Simulink model of open loop BBC	51

Figure 4.3 Open loop BBC's output voltage	52
Figure 4.4 Open loop BBC's inductor current.....	52
Figure 4.5 BBC's output voltage with GA-PID.	53
Figure 4.6 BBC's result with GA-PID in presence of input voltage and load resistance variation	54
Figure 4.7 BBC's output voltage with STSMC.....	55
Figure 4.8 BBC's output voltage with STSMC using staircase reference	56
Figure 4.9 BBC's simulation result with STSMC for varying load resistance and input voltage	57
Figure 4.10 BBC's output voltage of GA-STSMC, PSO-STSMC and GA-PID	59
Figure 4.11 BBC's output voltage of GA-STSMC, PSO-STSMC and GA-PID with staircase reference	60

LIST OF ACRONYMS

BBC	Buck-Boost Converter
CCM	Continuous Conduction Mode
DCM	Discontinuous Conduction Mode
DC	Direct Current
FOSMC	First Order Sliding Mode Controller
HOSMC	Higher order Sliding Mode Controller
GA	Genetic Algorithm
MOSFET	Metal oxide Semiconductor Field Effect Transistor
IGBT	Insulated Gate Bipolar Transistor
ITAE	Integral Time Absolute Error
PID	Proportional Integral Derivative
PSO	Particle Swarm Optimization
PV	Photo Voltaic
PWM	Pulse Width Modulation
SMC	Sliding Mode Control
SMPS	Switch Mode Power Supply
SMVC	Sliding Mode Voltage Controller
STSMC	Super Twisting Sliding Mode Controller

LIST OF SYMBOLS

C	Capacitor
C_{\min}	Minimum capacitance
C_1	Sliding Surface coefficient 1
C_2	Sliding Surface coefficient 2
C_3	Sliding Surface coefficient 3
D	Duty Cycle
f	Switching Frequency
i_c	Actual capacitor current
I_c	Average capacitor current
i_d	Desired current
i_L	Actual inductor current
I_L	Average inductor current
$I_{L\min}$	Minimum inductor current
$I_{L\max}$	Maximum inductor current
J_{\min}	Minimum cost function value
K_1	Gain constant 1 for STSMC
K_2	Gain constant 2 for STSMC
K_d	Derivative gain
K_i	Integral gain
K_p	Proportional gain

L_{\min}	Minimum inductor
L	Inductor
R	Load resistor
S	Switch
S	Sliding surface
T	Switching period
Q	Charge
v_c	Actual capacitor voltage
V_c	Average capacitor voltage
V_i	Actual input voltage
V_I	Average input voltage
V_L	Average inductor voltage
v_L	Actual inductor voltage
v_o	Actual output voltage
V_o	Average output voltage
V_d	Desired voltage
u_{eq}	Equivalent controller
Δi_L	Ripple inductor current
ΔV_o	Ripple output voltage

ABSTRACT

DC-DC converters efficiently and quickly transform a direct input voltage to regulated direct output voltage. Control of DC-DC buck-boost converters is challenging because of the nonlinearity in its dynamics and complexities in the system. Proportional Integral Derivative (PID) controller is frequently used to obtain the required output voltage from converter due to its simplicity. However, using a PID controller for non-linear systems is neither dependable nor satisfying. In this thesis, Super-Twisting Sliding Mode Controller (STSMC) is designed for such converter system based on Genetic algorithms (GA) and Particle Swarm optimization (PSO) methods. To compare the designed controller, GA-based PID controller was designed. The study begins by formulating the mathematical model of buck-Boost converter and defining its control objectives. The STSMC is then designed and implemented using MATLAB/Simulink software package. The STSMC is a robust control technique that offers fast transient response and high disturbance rejection capabilities. It is capable of yielding the desired voltage under uncertainties due to variations in input load, voltage and also the reference. Its performance is assessed by analysing its response characteristics, including settling time, overshoot, and robustness to disturbances. The simulation results demonstrate that the STSMC achieves excellent voltage control performance for the converter. In line with this, the PSO based STSMC has settling time for 0.3108msec, rise time for 0.19573msec and overshoot for 0.1402%. On the other hand, the PSO based STSMC for voltage control has improved performance than GA based STSMC and GA-PID controller. The proposed control systems are compared based on performance analysis. Additionally, under the influence of an external disturbance, the effectiveness of controllers is assessed. Finally, PSO based STSMC controller was acceptable rather than GA based STSMC and GA-PID controller for voltage control of the proposed system.

Keywords: - Buck-Boost converter, STSMC, DC-DC Converters, GA, PSO-STSMC, PID

CHAPTER ONE

INTRODUCTION

1.1 Background of the study

A substantial amount of power is required for the everyday activities of consumers. With the desire for power, technology is constantly evolving. As the population of world increases, so does the need for electricity. Modernizing traditional power producing methods is necessary to overcome this problem. According to renewable energy sources, modern power electronic components are being used to address the issue of the energy crisis. These resources seem advantageous in case of load-shifting, max-power generation, consumer and demand (Gitleman, 2014).

It is uncommon to use electric power or power condition control in the same way that it was produced or distributed. Several different power electronics circuit types are used to transfer electricity from a supply to a load. The DC-DC converter is one of the most significant varieties. The most common power electronic module for these applications are buck-boost converters.

Only the most common passive and active components are used in the buck-boost converter with load (Gitleman, 2014). Consequently, it is renowned for being simple to use. In addition to all of these advantages, buck-boost converter non-linearity factors like delay and hysteresis also contribute for load changes, power in switching, transients, and electromagnetic interference. These problems are resolved and performance is maximized for effective power management using various linear and non-linear controller types.

Electronic circuits called DC-DC converters change a direct source's (DC) voltage range from one range to other. They are the power electronics circuits that are most frequently used. Nowadays found in almost all electronic gadget, semiconductor components are powered by DC supplies. In all situations where stabilizing input DC voltage to set point is required, they are primarily used (Gaussian Fuzzy Logic Control, 2012).

One of the most crucial converters is the buck-boost converter. The output voltage that is either lower or greater than the input voltage characterizes this switched-mode power source. It is referred to as inverting converter as the output voltage's polarities is the opposite to that of the input voltage. These converters are typically utilized in industrial applications and are specifically helpful for photo voltaic maximum power tracking and used as DC transformer.

There are typically two modes of operation for these converters: discontinuous and continuous. In continuous mode, the output current doesn't drop to zero. As the switch is turned-off on discontinuous mode, then the output current zeroes out (M. Theses and R. Citation, 2017).

Switch-mode power sources typically employ DC-DC converters. they are becoming more and more common in numerous industries. This is a result of their diverse variety of uses, which include, among others, DC motor drives, power supply for automobiles, airplanes, telecommunications equipment, office equipment, computers, and appliance control (padhyay et al., 2015). Numerous kinds of DC-DC converters are there. The widely well-known converters are buck converters, boost converters, and buck-boost converters. Voltage stepdown/reduction is accomplished by the buck converter, voltage step-up is accomplished by the boost converter, and voltage step-up or step-down is accomplished by the buck-boost converter.

DC-DC converters are necessary for all voltage level like low, medium, and high power application. In addition, DC-DC converters are frequently applied to regulate electrical drives, one of that is the regenerative braking of DC motors, which recycles energy back into the source (Hussein et al., 2015).

The output voltage of DC-DC buck-boost converter is typically not stable due to the functioning of switching components. Because they are straightforward, linear controllers have been utilized in this converter to achieve constant, steady output voltage, however they are unable to deliver the optimal outcomes when combined with nonlinear systems. Nonlinear control techniques are still in demand because they consistently deliver the finest outcomes. In this thesis, an optimal super twisting sliding mode controller had been designed for DC-DC buck-boost converter to produce stable and steady output voltage with quick response time.

1.2 Statement of the Problem

DC-DC converters, such as buck-boost converter, rely on power semiconductor components which act as electronic switch. The nonlinear behaviour of these converters stems from the operation of these switching devices. The buck-boost converter, in particular, often exhibits unstable and oscillatory behaviour, with significant overshoot and a prolonged settling time for its single output voltage. Moreover, it struggles to maintain the desired voltage when there are variations in the input voltage and load. To address these challenges,

a controller with a high level of dynamic response is necessary for the buck-boost converter. While PID controllers have traditionally been used due to their ability to achieve the desired voltage, they are not reliable or effective for nonlinear systems like the buck-boost converter. Incorporating system parameter variations and achieving fast response times are challenging with PID controller implementations, leading to extended rising and settling times that impact voltage regulation. To enhance the performance of buck-boost converter, an optimal STSMC has been developed in this thesis. Optimization techniques namely PSO and GA have been employed to attain optimality in the controller design. This approach has resulted in improved converter performance by mitigating the issues associated with voltage regulation.

1.3 Objectives of the Study

1.3.1 General Objectives

The general objective of this thesis is to design an optimal super twisting sliding mode controller for voltage control of a DC-DC buck-boost converter and improving robustness under input and load variation.

1.3.2 Specific Objectives

- To analyse the performance and robustness of STSMC for voltage regulation of the converter.
- To tune the parameter of the designed controller STSMC with different optimization techniques.
- To perform the simulation based on system dynamical model.
- To examine the effectiveness of the proposed controller compared to PID controller which includes operating point, input voltage and load variations.
- To demonstrate better results, conclusions and recommendations resting on system outcomes.

1.4 Scope of the Study

The scope of this research includes determining the mathematical model of the proposed system dynamics, designing PID, GA and PSO based STSMC for voltage control of the DC-DC buck-boost converter. The performance of these controllers is examined in terms of settling time, maximum overshoot, rise time, and voltage variations from required values

under input voltage and load variations. The system dynamics is applied in MATLAB/Simulink to analyse the converter's parameters and responses.

1.5 Limitations of the Study

The study is confined to run simulation for the system with MATLAB/Simulink and displaying the interactions between the system's various parameters. This is because building a real system requires a number of difficult-to-find components. Additionally, it calls for spending more time and money on developing the prototype and its implementation.

1.6 Significance of the Study

The value contributed and how it enhances the current process are how any control research is evaluated. The improvement of performance indices for this converter system, such as overshoot, settling time and rising time is the intended outcome of this thesis. The importance of this research is that it will advance the quality of systems or devices that employ buck-boost converters.

1.7 Thesis Organization

The thesis is organised as:

Chapter one: The broad backdrop of the study is outlined in this chapter. The problem statement, scope, significance, objective, employed to finish the thesis, then its organization are only a few of the analysis's most crucial components that are covered in this chapter.

Chapter two: Presents literatures reviews of previous research work.

Chapter three: Presents information generally based on the DC-DC buck-boost converter, and also methods and materials, and mathematical modelling of the system. In this chapter, the controller design (STSMC and PID) and optimization methods like GA and PSO is presented.

Chapter four: Present result and discussion on the outcomes.

Chapter five: Present Conclusion and recommendations based on the outcomes.

CHAPTER TWO

LITERATURE REVIEW

2.1 Related Work

Electronic converter plays a crucial function in converting voltage from one level to another. One of the most popular and effective power electronics circuits for converting uncontrolled electrical voltage from one level to desired regulation is DC-DC switching type converter. Switch mode is controlled using a variety of control techniques. The majority of industrial and high-performance applications always have a need for DC-DC converters and the straightforward, inexpensive controller structure. Every control mechanism has some merit and demerit as a result of which it is regarded as an appropriate control method under particular circumstances whenever compared to other control mechanisms. The best control strategy, regardless of the situation, is often in demand.

(Almawlawe & Kovandzic, 2016) put Modified Method for Tuning PID Controller of Buck-Boost Converter. Such work suggests design and modelling of more straightforward method for creating a PID controller for the CCM of buck-boost converter. The method works well for controlling voltage and was appropriate for the buck-boost converters, but it is prone to substantial fluctuations which could cause the system to stray from ideal situations as a result of line changes and input parameter changes. These PID controllers are suitable for Buck-Boost applications and provide good voltage regulation, according to simulation findings. The acquired findings show the proposed reliability of controller, and the converter output was examined (Almawlawe & Kovandzic, 2016).

(R. Marouani, K. Echaieb, 2012) found that SMC for buck-boost converter on pv grid system. In order to catch the desired voltage needed by the main grid, this converter is managed by the sliding mode control (SMC). A DC bus and a three-phase voltage inverter make up the second stage, which connects the GPV to the grid utility. With the help of the SMC, the dc-dc controller is able to track the desired direct voltage that the grid demands. Injecting a three-phase equilibrated current system having small harmonic noise into the grid is made possible by direct power control used on the inverter.

(Algamluoli, 2020) has presented the voltage control of buck-boost converter using PID Controller. PID controllers for buck boost converter output voltage and load current are constructed and investigated. As a result, buck boost converter was created and put into use

to enhance how quickly the system reached steady state following the creation of PID controllers for current and load voltage (Algamluoli, 2020).

(Verma, 2018) has suggested dc-dc boost converter with SMC under different conditions. This research used SMC with changed parameter values and a beta factor for accurate values in a feedback, closed-loop system to overcome this challenge. Under varying circumstances, the input source is used to be a dc source voltage. The dynamic behaviour of the system is not essentially influenced by variation under operation condition because the settling time for SM controllers is practically constant and is approximately 3.4 milliseconds for varying loads (Verma, 2018).

(Al-Qaisi et al., 2019) has proposed high performance buck converter(dc-dc) with SMC. In the proposed approach, a buck converter is developed using PW modulation based on PID SM voltage controller, and the response for suitable control settings has been measured. The performance characteristics have been evaluated and assessed for system stability, which clearly demonstrates that the buck converter, which is stabilized by a SMC, have a quick dynamic reaction and is effective in different application.

(Teja et al., 2012) presented a SMC for a Buck Converter operating in continuous conduction mode, which is optimized using particle swarm optimization. The main objective of this optimized controller is to achieve a rapid response under different operating conditions. Simulation results confirm its effectiveness in handling variations in line and load conditions. The study concludes that conventional controllers for Buck converters tend to produce inadequate dynamic behaviour due to changes in the operating point. To overcome this limitation, the feedback controller identification problem is treated as an optimization task using a modified PSO technique. The proposed controller surpasses a PSO-based controller in terms of performance and demonstrates robustness.

(Abderrezek & Harmas, 2014) presented an adaptive non-singular terminal sliding mode (ANTSM) tracking control is introduced for a DC-DC buck converter. The control method incorporates adaptive law to estimate parameter uncertainty and external disturbance, ensuring robustness. Terminal sliding mode control (TSMC) guarantees finite-time convergence of the output voltage error, while Particle Swarm Optimization (PSO) optimizes control parameters for improved performance. Simulation results confirm the effectiveness of this approach in maintaining dynamic and steady performance even in the presence of load variations and disturbances. The integration of TSMC and adaptive disturbance

estimation successfully overcomes unknown disturbances, while the use of PSO reduces chattering and facilitates faster convergence compared to conventional methods.

(Guldemir, 2011b) examines the development and analysis of a robust SMC for a DC-DC buck converter. The paper derives the dynamic equations of the buck converter and designs a sliding mode controller. A two-loop control strategy is implemented for the converter. Through simulations, the robustness of the SMC system is evaluated by considering step load changes and input voltage variations. The simulation results indicate a rapid dynamic response of the output voltage and resilience to load and input voltage fluctuations. The review concludes that the sliding mode controlled buck converter successfully tracks the desired output voltage, exhibits robustness against load disturbances and input voltage variations, and maintains stable operation even when subjected to significant supply and load variations.

(Tolossa, 2017) mentions that DC-DC buck converters are commonly used for voltage step-down applications but often exhibit instability, oscillations, overshoot, and long settling time. PID controllers have traditionally been employed for controlling these converters due to their simplicity, but they are not reliable for nonlinear systems. To address these issues, the literature proposes the use of a second-order sliding mode (SOSM) controller based on the prescribed convergence algorithm. The performance of the SOSM controller is compared with that of the PID controller in terms of dynamic response, including overshoot, settling time, rise time, and voltage deviation, using MATLAB/Simulink. Simulation results demonstrate that the SOSM controller outperforms the PID controller by improving rise and settling times and completely eliminating overshoot. Furthermore, the SOSM controller effectively handles variations in load resistance and large input voltage fluctuations, ensuring the output voltage remains close to the desired value. Overall, the literature concludes that the performance of the SOSM controller is superior to that of the PID controller.

(Mekonnen, 2019) focuses on the control of switched-mode DC-DC converters, which are widely utilized due to their efficiency and versatility in providing adjustable output voltages. However, these converters often suffer from instability, oscillations, and lengthy settling times. To overcome these challenges, advanced control methods are necessary. This study proposes the use of a Fuzzy PID controller and an integral sliding mode controller, both designed to achieve stable and rapid performance for a buck-boost converter. The controllers are evaluated through simulations in MATLAB/Simulink, considering performance indexes such as integral square error, integral absolute error, integral time square error, and integral

time absolute error. Additionally, the controllers are tested under varying load resistance and external disturbances. The research underscores the significance of obtaining consistent and swift system responses in DC-DC converters, with keywords including DC-DC Converter, Buck-Boost Converter, Integral SMC, and Fuzzy PID Control.

(Nugusa, 2021) explores the utilization of switch-mode DC-DC converters, which efficiently convert DC input voltage into regulated DC output voltage. Advanced control methods have been developed to address the need for precise control in these converters. However, challenges such as output voltage oscillation, overshoot, and slow settling time persist, particularly during input voltage and load variations. To enhance performance, this study proposes GA, GA-Fuzzy, and sliding mode controllers for buck-boost converters. Simulations demonstrate that GA-fuzzy control achieves swift output voltage response, while sliding mode control exhibits longer settling times. The proposed controllers effectively mitigate overshoot and undergo performance comparisons. Their resilience towards input voltage and resistance fluctuations, as well as their capability to handle random external disturbances, are assessed.

2.2 Summary of Literature

The research highlights the limitations of PID controllers in dealing with fluctuations caused by line and input parameter changes. The application of SMC in grid systems successfully achieved the desired voltage and injected balanced current into the grid. The utilization of PID controllers improved the steady-state response for voltage and load current control in buck-boost converters. By adjusting parameter values and incorporating a beta factor, SMC demonstrated accurate feedback control in varying conditions. A high-performance buck converter employing SMC based on PW modulation exhibited quick dynamic response and effectiveness in diverse applications. The optimization of SMC using particle swarm optimization enhanced performance and robustness in buck converters operating in continuous conduction mode. The integration of adaptive non-singular terminal sliding mode (ANTSM) tracking control, fuzzy PID, and integral sliding mode controllers achieved fast and stable performance. Second-order sliding mode (SOSM) controllers, designed based on the prescribed convergence algorithm, improved rise and settling times while eliminating overshoot in DC-DC buck converters. Lastly, the use of fuzzy PID and integral sliding mode controllers demonstrated stable and rapid performance under load resistance variations and external disturbances in buck-boost converters. Overall, the reviewed studies indicate the

superiority of advanced control methods over traditional PID controllers in terms of dynamic response and robustness in DC-DC buck-boost converters.

Generally, considering the literature reviewed, the SMC designed in the reviewed papers didn't consider chattering effect, and the controllers designed by PID have long settling and rising time that decrease system efficiency and the robustness of the controllers were not been discussed for different staircase reference. So, Optimal PSO and GA based STSMC has been carried out in this research work to override such gap.

2.3 System Overview

Electronic components known as DC-DC converters alter the voltages of DC electrical power. They transmit energy using inductor and capacitor as energy storing devices (Guldemir, 2011a). Switched-mode power supply (SMPS), the DC-DC converters are often used so as to have numerous uses. They are becoming more and more important in everyday life. Different converter types exist. The widely well-known ones are boost, cuk, buck, and buck-boost converter.

2.3.1 DC-DC Buck-Boost Converter

Buck-boost converter, which belong to the category of switched mode power supplies, integrate the principle of buck converters and boost converters into simple one circuit. Buck converters are mostly employed in power supply to generate direct current (DC) outputs within a voltage range starting from 0 volts and slightly below the input voltage. On the other hand, the boost converters have a broader scope of potential voltage variations, extending from the input voltage to significantly higher level than the input (L. Guo, V. Nelson, R. Nelms, J. Hung, 2006).

In various applications, especially those involving battery-powered devices, the input voltage can change necessarily. For instance, it may begin at fully charged state and gradually decrease when the battery charge is dropped. In situations where the battery voltage exceeds the required voltage for the circuit, a buck regulator is the optimal choice as it maintains a constant supply voltage corresponding to the full charge.

However, as the battery charge diminishes, the input voltage drops below the circuit's necessary level, necessitating an alternative solution. This is when a boost regulator, as described by (L. Guo, V. Nelson, R. Nelms, J. Hung, 2006) becomes the preferred option.

The boost regulator ensures that the circuit receives the voltage it requires, even when the battery charge is low, by either draining or replenishing the battery.

After careful consideration, it was determined that a buck-boost converter would be the most appropriate choice. This kind of converter finds frequent application in energy management scenarios, but it introduces nonlinearities to the system due to modifications in components like capacitor and inductor. As a result, traditional linear control methods are not practical for direct evaluation. One notable characteristic of the buck-boost converter is that its output voltage could either be more or less than the input voltage. Additionally, polarity of the output voltage is always against to the input voltage, leading to its classification as an inverting converter.

A typical inverting, non-isolated power stage topology is the buck-boost, also referred to as a step-up or down power stage. Since the output voltage is inverted from the input value and could either be higher or lesser than the input voltage, buck-boost energy steps are selected by power source designer. The output voltage of the topology is either two orders of magnitude more (boost energy stage) or lesser (buck energy stage) than the input voltage, hence the name of the topology (Shamim-Ul-Alam et al., 2010).

Enhancing energy efficiency conversion is a primary objective for electronic engineers. In the case of PWM converters, minimizing switching losses is a critical performance parameter. In the CCM of a buck-boost converter, there exist two states during the switching period. When a transistor is turned on, it is considered to be in the ON state, while the diode operates in an OPEN circuit mode. Conversely, when the transistor is turned off, it is in OFF state, and the diode operates in a CLOSE circuit mode. Each of these states could be represented by easy linear circuit, with appropriate circuit configuration serving as the switches for the respective states.

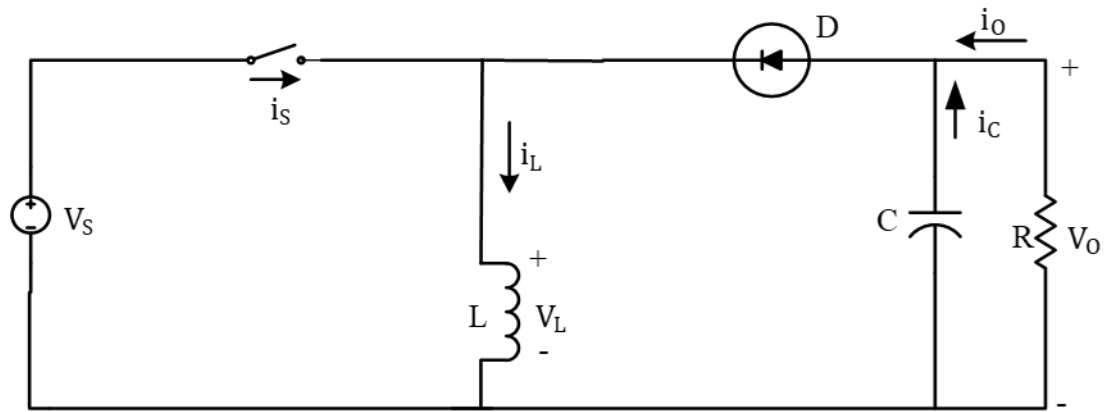


Figure 2.1 BBC's circuit (Guldemir, 2011a)

The length of time during which the transistor is in the ON state is determined by the duty cycle, labelled by D , and stated as a ratio of the switch ON time (T_{on}) to the total time of single complete switching cycle (T_s), which is typically 0.01 milliseconds. The duty cycle has been set by the control circuit. On the other hand, the period during which the transistor is in the OFF state is referred to as T_{off} . In CCM, so as there are only two states per switching cycle, T_{off} can be computed as $(1 - D)$ multiplied by T_s . The amount $(1-D)$ could be represented as D' (Gaussian Fuzzy Logic Control, 2012). Figure 2.2 displays the waveform of the converter operating under CCM.

Handheld electronics, many industrial processes, and alternative and renewable energy conversion all rely on converter. It is typically used to transform a non-regulated dc source to a controlled DC voltage, such as output of rectifier and battery. Notwithstanding, only within a certain range does the source drastically vary due to changes in line voltage, a battery running out, etc. With all of this in mind, the goal is to transmit power to a wide range of loads while maintaining a consistent voltage.

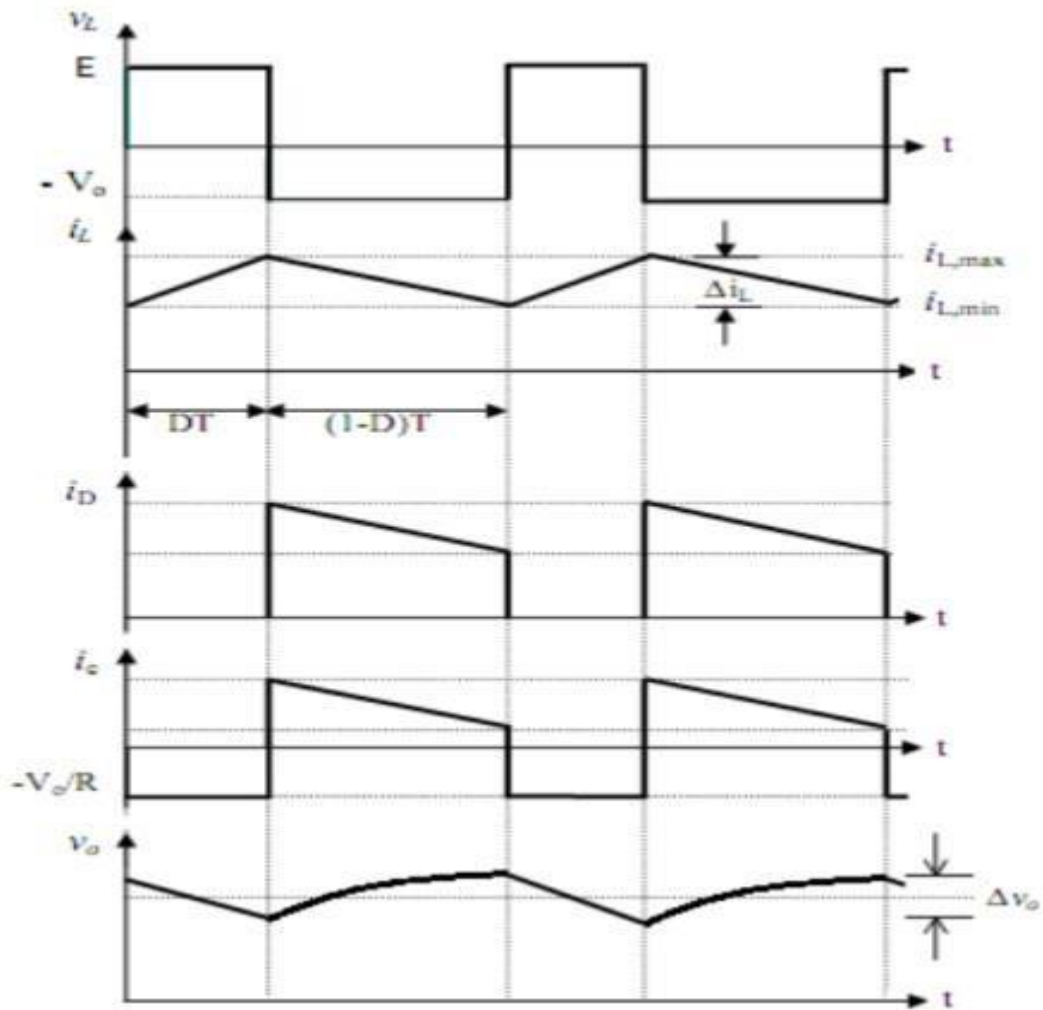


Figure 2.2 The waveform of BBC during CCM (Guldemir, 2011a)

2.3.2 Mode of Operation of Buck-Boost Converter

DC-DC buck-boost converter typically works in two modes depending on the continual flow of inductor current. The modes include: Discontinuous conduction mode (DCM) and Continuous conduction mode (CCM)

CCM and DCM are terms used to describe the behaviour of current in the power storing component (inductor) within every switching cycle. CCM refers to a situation in which the inductor current doesn't reach zero, ensuring that there be always energy remaining at the last of every cycle. This remaining energy is replenished in the subsequent cycle to give power to the output.

On the other hand, under DCM, the inductor experiences periods where it has no current and no stored energy because each cycle consumes all available energy. Whether a converter

operates in CCM or DCM depends on the load conditions (M. Theses and R. Citation, 2017), which is proportional to the quantity of the energy accumulated.

2.3.3 Continuous Conduction Mode

In situations where the current flowing along the inductor does not drop to zero, this inductor undergoes partial discharge prior to the beginning of each switching cycle. This happens as the current flow through the inductor remains continuous during both the charging and discharging phases. In CCM, every switching cycle could be bisected into two parts: $D'T$ and DT , where D and D' add up to one. In the first mode, DT , the inductor current rises, while in the second mode, $D'T$, the inductor current fall down. Figure 2.3 shows the waveform of inductor current during CCM.

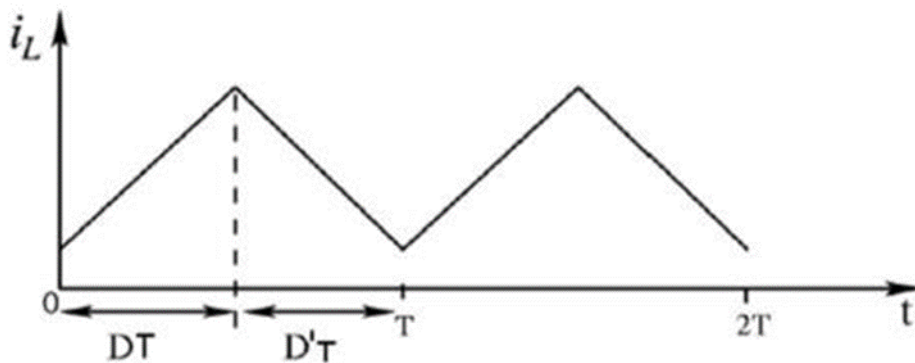


Figure 2.4 The waveform of inductor current during CCM (padhyay et al., 2015)

2.3.4 Discontinuous Conduction Mode

By the wrap-up of a switching cycle in the DCM, the current passing along the inductor reaches zero, notifying that the inductor is completely dis-charged. Within each switching cycle, there is a prolonged period where the inductor current remains at zero without any charge or discharge. In the DCM, every switching cycle can be bisected into three parts: $D'T$, DT , and $D''T$, where D , D' , and D'' add up to one.

In the first mode, DT , the inductor current rises, while in the second mode, $D'T$, it falls down. In the third mode, $D''T$, the inductor current remains null without any charge as well as discharge taking place. Figure 2.5 shows the waveform of inductor current during DCM.

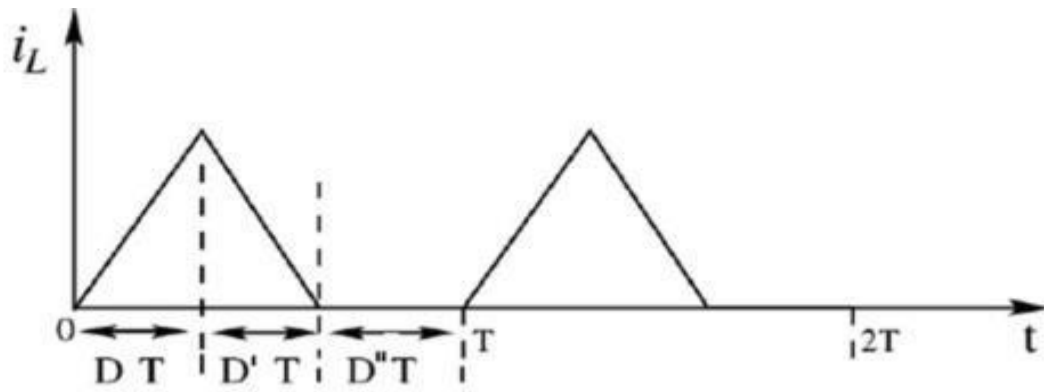


Figure 2.6 The waveform of inductor current during DCM (padhyay et al., 2015)

2.3.5 Functions of Various Buck-Boost Converter Components

The buck-boost converter uses a variety of components, that are: Inductor, Capacitor, Diode and Switch

A. Inductor

The inductor's task is for controlling the current slew rate via the power switch whenever the circuit is turned on. The inductor's current can't quickly change direction. An inductor functions as a source to maintain current flow when the current through it starts to decline. The inductor's ability to retain energy while lowering voltage is its greatest advantage. Additionally, the inductor determines if the converter is operating in CCM and keeps track of the ripple percentage. A faster transient response is made possible by the lower inductor value, but at the expense of more current ripples and large conduction losses in the switch and inductor. For the purpose of reducing output voltage ripple, a smaller inductor also calls for a bigger filter capacitor. Frequently wrapped around toroidal cores with a dispersed air gap to store power, ferrite or powdered iron toroidal cores are used to create switched supply inductors.

B. Capacitor

An energy storage system is employed to fulfil the filtering role of the capacitor by giving pathway for harmonic currents to bypass the load. To mitigate voltage overshoot and minimize ripple on the output of buck-boost converter, the presence of output capacitance over the load is necessary. Due to the capacitor's size, the voltage remains relatively stable as the switch is in off state, resulting in minimal voltage fluctuations.

C. Diode

Since the inductor current cannot abruptly change, it must have a direction even while the switch is turnoff. This direction is given by the freewheeling diode. Its use is not to correct the circuit; rather, it is to direct current flow and make certain that current usually flows into the inductor. The ability of this diode to swiftly shut off is also crucial. The diode permits for the converter able to now send the inductor stored energy for load. Because of this, DC-DC Converters have a better efficiency than a linear regulator. In a linear fashion, the current rises as the switch are closed. The freewheeling diode generates linear decrease to current as the switch is opened.

D. Switch

The purpose of the switch in the converter is to change its configuration. When the switch is turned on, the inductor generates and stores energy. On the other hand, when the switch is turned off, the stored energy is transferred to the load. In a simple way, switch could be represented by a dial switch that alternates b/n the source voltage and ground. Switching power supplies require transistors that possess fast switching speeds and can withstand voltage spikes that occur due to the inductor. These transistors are necessary to ensure efficient operation and control in the switching process. The widely common switching components are the GTO, SCR, IGBT, and MOSFET. Efficacy MOSFETs play a significant role in large frequency power systems, including large density power supply (Rahman, 2007). As a result, MOSFETs are utilized in systems with considerably lower voltages and higher frequencies.

Frequency of Operation

The switching frequency of a converter is determined by the frequency that the switching port is switched off and on. Generally, the switching frequency span from some kilohertz to some megahertz (e.g., 20 kHz to 2 MHz). Increasing the switching frequency has the advantage of reducing the number of key components like inductor, resistor and capacitor. Additionally, it allows for more compact designs on the circuit board and in the overall case, optimizing space utilization.

According to (Rahman, 2007) This frequency affects the choice of component: like Physical sizes decrease as frequency increases, frequency response, power losses minimum on-time, electrical traits and other factors. The operation of switch frequency affects the output. In research and innovative power converter design, increased switching frequencies are becoming more and more common.

CHAPTER THREE

MATERIALS AND METHODS

3.1 Chapter Overview

This chapter discusses mathematical modelling and controller design of the DC-DC buck-boost converter and also includes data gathering and analysing. This converter is nonlinear; therefore, linear controllers are not able to provide the optimal output against required load and voltage variations. Nonlinear SMC had been designed for buck-boost converters to address the drawbacks of linear controllers. Finally, MATLAB is used to simulate the system.

3.2 Materials used

MATLAB/2019, Microsoft Office 2016, and MathType 7.0 equation were used for the research work. A software program called MATLAB comes with Simulink and technical toolboxes. In Microsoft Office, the thesis documentation is revised. The mathematical equations and formulae can be written using the presentation tool MathType 7.0 for Microsoft Word and PowerPoint.

3.3 Methods

The achievement of this thesis has been achieved using the following technique:

- **Literature review:** This section will investigate the control methods of the buck-boost converter. A thorough examination of relevant literature concerning this thesis work has been conducted, including an in-depth analysis of their respective control mechanisms.
- **System modelling:** This section is set to establish modelling of the proposed system, including its mathematical representation.
- **Controller designing:** The subsequent phase involves creating a controller. By employing different optimization techniques such as PSO and GA, the system selects the most effective controller and adjusts its parameters accordingly.
- **Simulation and Analysis:** In this phase, the system will be simulated using MATLAB/Simulink simulation tools. This simulation step aims to evaluate and analyse the potency of the system.

- **Documentation and conclusion:** This part do comparisons between the controllers, enumerates the results, and wraps up the study after simulating the proposed models. To complete this thesis, the following procedures are undertaken, and the entire process is depicted in the diagram on Figure 3.1.

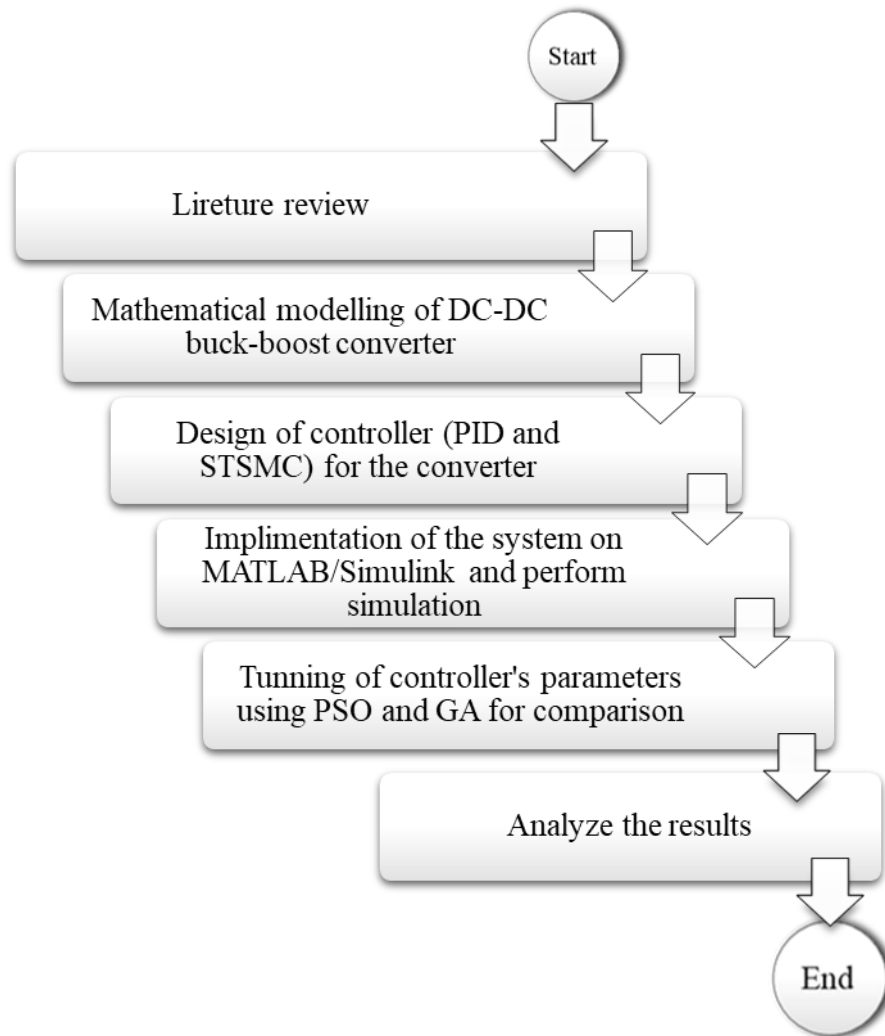


Figure 3.1 Block diagram of the research methodology

3.4 Block diagram of the research work

The block diagram of the control system of the proposed BBC system is depicted in Figure 3.2. In SMC, the controller utilizes a sliding surface to determine the input state, $U(t)$, for the system. In the case of SMC, the switching state, $U(t)$, that determine the activation and deactivation of the converter switches, are determined by the sliding line.

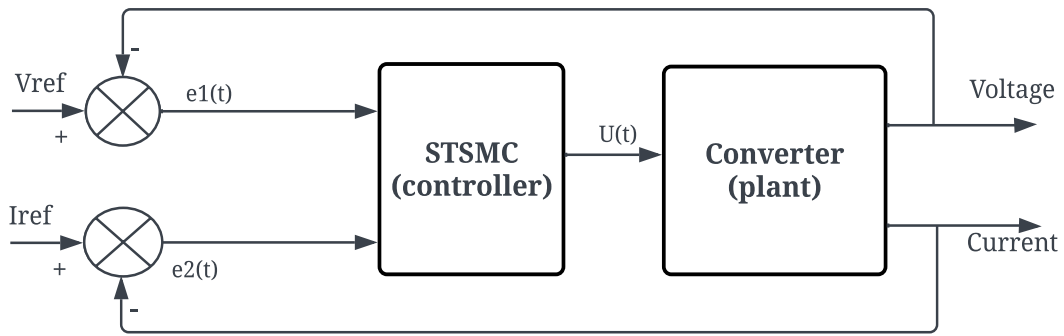


Figure 3.2 Block diagram of the research work

3.5 Analysis of Buck-Boost Converter

By applying Kirchhoff's current and voltage law, the analysis of the converter system allows for the measurement of the following parameters as the switch is close or open.

3.5.1 Calculation of duty ratio

To estimate the duty ratio, begin by supposing that the converter is in a stable state. It is crucial to acknowledge that this review assumes an ideal scenario and does not consider any parasitic resistances. Moreover, the research supposes that the converter works solely in CCM, meaning that the inductor current is non-zero. Analysing a two-state converter is necessary to determine the duty ratio.

3.5.2 Converter Analysis when the Switch Closed

Below is a diagram of the converter's associated circuit as the switch closed.

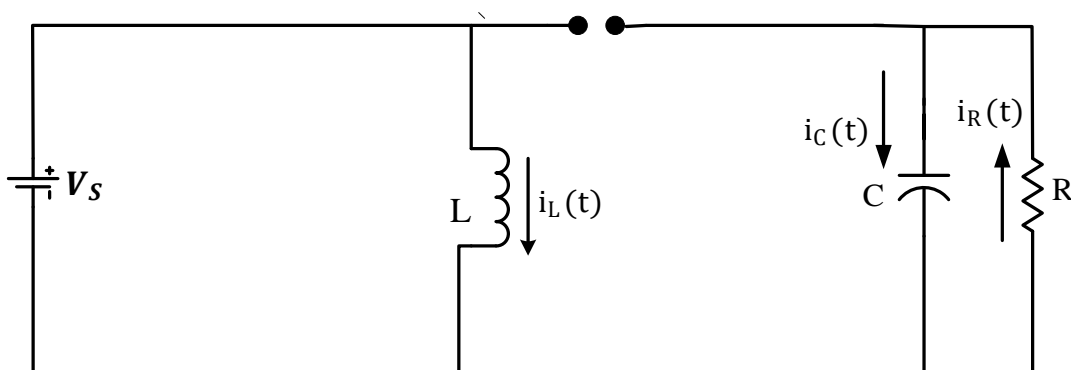


Figure 3.3 Circuit for the converter as the switch is closed

The diode will be reverse bias as the switch is kept closed for an extended period of time. Positive voltage is thus generated across the inductor.

$$V_s = V_i = L \frac{di_L(t)}{dt} \quad (3.1)$$

It is possible to express Equation (3.1) as follows:

$$\frac{\Delta i_L}{\Delta t} = \frac{V_i}{L} \quad (3.2)$$

The time duration that the switch is 'on', it is provided as: $\Delta t = DT$, equation (3.2) is presented as follows.

$$\Delta i_L(\text{closed}) = DT \left(\frac{V_i}{L} \right) \quad (3.3)$$

3.5.3 Converter Analysis for the Switch Open

The accompanying diagram illustrates the buck-boost converter's comparable circuit as the switch opens and the diode is forward biased in the conducting condition. Figure 3.4 shows the circuit for the converter as the switch is open.

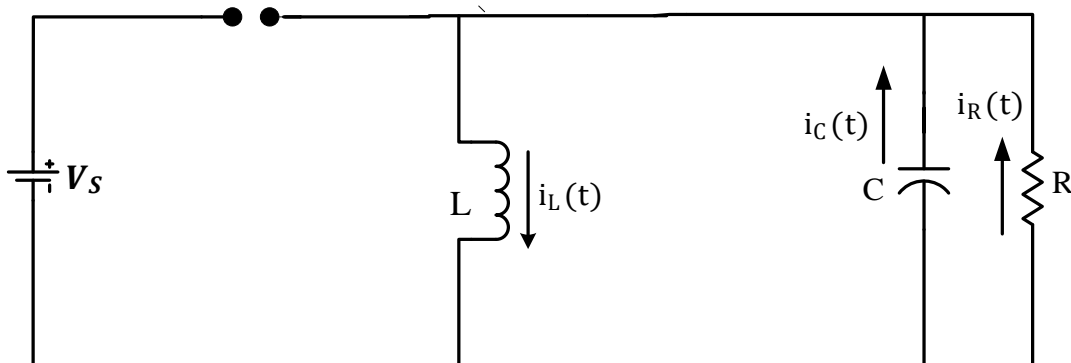


Figure 3.4 Circuit for the converter as the switch is open

Inductor current progresses to flow as the switch becomes off due to the inductive energy stored. Since the diode is currently forward biased, current passes via it.

$$L \frac{di_L(t)}{dt} = V_o = -V_C \quad (3.4)$$

Equation (3.4) has the following possible forms:

$$\frac{\Delta i_L}{\Delta t} = \frac{V_o}{L} \quad (3.5)$$

Since $t = (1 - D)T$ represents the amount of duration at which the switch is off, Equation (3.5) is expressed as,

$$\Delta i_L (\text{open}) = -\frac{(T - DT)}{L} V_o \quad (3.6)$$

For steady state functioning, net difference on inductor current during a period should be zero.

$$\Delta i_L (\text{open}) + \Delta i_L (\text{closed}) = 0 \quad (3.7)$$

Equation (3.7) is altered to equation (3.8), which is then simplified, by inserting Equations (3.3) and (3.6).

$$D = -\frac{V_o}{V_i} (1 - DT) \quad (3.8)$$

By solving for V_o , we can obtain

$$V_o = -V_i \frac{D}{(1 - D)} \quad (3.9)$$

Equation (3.9) illustrates the output voltage supplied by the BBC in relation to the input voltage. The system produces three phases of voltage based on the duty cycle (Gaussian Fuzzy Logic Control, 2012).

- As the duty cycle is larger than 0.5, output voltage of the system becomes larger than the input voltage, indicating that the system is operating in boost mode.
- As the duty cycle is equal to 0.5, the system's output voltage becomes identical to the input voltage.
- As the duty cycle is lower than 0.5, the system's output voltage becomes lesser than the input voltage, indicating that the system is operating in buck mode.

The converter does not directly connect the supply to the load. Instead of it, energy is transferred to the load by keeping it on the inductor as the switch is closed and then delivering it as the switch is open. As a result, the BBC is often called indirect converter.

On steady state operation, inductor voltage's integral (V_L) on a single duration period must be zero, ensuring that the waveform repeats from single time period to the next.

$$\int_0^T V_L dt = \int_0^{t_{ON}} V_L dt + \int_{t_{ON}}^T V_L dt = 0 \quad (3.10)$$

Integrating over T, the switching time ($T = t_{ON} + t_{OFF}$), yields

$$t_{ON}(V_i - V_o) = (T - t_{ON})V_o \quad (3.11)$$

Equation (3.11) may be condensed to this form as:

$$D = -\frac{V_o}{V_o}(1-D) = (1-D)\frac{t_{ON}}{T} \quad (3.12)$$

3.5.4 Inductor Calculation

In the absence of power loss in the converter, the load is needed to use equal amount of power as the supply.

$$P_o = P_s \quad (3.13)$$

Equation (3.13) can be written as,

$$\frac{V_o^2}{R} = V_i I_s \quad (3.14)$$

$$I_s = I_L D \quad (3.15)$$

There is a proportionality between average supply and inductor current as seen on equation (3.15)

Using above equation, equation 3.14 could be expressed as,

$$\frac{V_o^2}{R} = V_i I_L D \quad (3.16)$$

The following is how to solve I_L for Equation (3.16):

$$I_L = \frac{V_o^2}{V_i D R} = \frac{P_o}{V_i D} \quad (3.17)$$

$$I_L = \frac{V_s D}{R(1-D)^2} \quad (3.18)$$

The constant current state requires that I_L to be bigger than ΔI_L .

The highest(max) and lowest(min) inductor current are as follows:

$$I_{L\max} = I_L + 0.5 * \Delta I_L \quad (3.19)$$

$$I_{L\min} = I_L - 0.5 * \Delta I_L \quad (3.20)$$

The following equation is obtained by simplifying and replacing for ΔI_L and I_L from equations (3.18) & (3.3) to equations (3.19) & (3.20), respectively as,

$$I_{L\max} = \frac{V_s D}{R(1-D)^2} + \frac{V_i DT}{2L} \quad (3.21)$$

$$I_{L\max} = \frac{V_s D}{R(1-D)^2} - \frac{V_i DT}{2L} \quad (3.22)$$

The boundary between CCM and DCM mode is thus established by setting the minimum inductor current to zero. Continuous current cannot flow unless the inductor current is positive.

Consequently, by rearranging equation (3.22) and solving for the inductor, one can determine the measure of the inductor that sets boarder b/n CCM and DCM.

$$L_{\min} = \frac{(1-D)^2}{2f} R \quad (3.23)$$

Here, f represents the reciprocal of T , which stands for switching frequency

This inductor value establishes the separation between CCM and DCM during operation. In order for the BBC system to work under CCM, the value of the inductor utilized in, it might be bigger than the minimum value of inductor.

The variation between the highest and lowest values of the inductor current is referred to as the ripple inductor current.

$$\Delta I_L = I_{L\max} - I_{L\min} \quad (3.24)$$

Equation (3.25) is formed by simplifying and replacing $I_{L\max}$ and $I_{L\min}$ from equations (3.21) & (3.22).

$$\Delta I_L = \frac{V_i DT}{L} \quad (3.25)$$

3.5.5 Capacitor Calculation

It is anticipated that the output capacitor will have a sufficient capacity to ensure stable output voltage. Nevertheless, ripple in the output voltage (ΔV_o) could be calculated by considering a realistic capacitance value and utilizing the waveform provided in the above figure for CCM. The maximum change in charge accumulated in the filtering capacitor is equivalent to the triangular area if the complete ripple part of the inductor current (ΔI_L) passes via the capacitor while the average current passes along the load (Safari, 2012).

$$\Delta V_o = \frac{\Delta Q}{C} \quad (3.26)$$

$$\Delta Q = \frac{1}{2} \frac{T}{2} \frac{\Delta I_L}{2} \quad (3.27)$$

Equation (3.27) is replaced as to produce equation (3.26).

$$\Delta V_o = \frac{1}{2} \frac{1}{C} \frac{T}{2} \frac{\Delta I_L}{2} \quad (3.28)$$

By rearranging the equations and substituting the values for ΔI_L from Equation (3.25) into Equation (3.28), it is possible to solve for the capacitor.

$$C_{\min} = \frac{(1-D)V_o}{8\Delta V_o L f^2} \quad (3.29)$$

The minimum required capacitance can be determined based on specific criteria such as preventing voltage overshoot and maintaining peak value of the ripple voltages under the given threshold. However, for achieving these objectives, the filter capacitance should be larger than the lowest required capacitance.

The output ripple voltage of the converter can be calculated as follows:

$$|\Delta Q| = \frac{V_o}{R} DT = C\Delta V_o \quad (3.30)$$

Solve for ΔV_o ,

$$\Delta V_o = \frac{V_o}{RC} DT = \frac{V_o}{RCf} D \quad (3.31)$$

As a result, having this

$$r = \frac{\Delta V_o}{V_o} = \frac{D}{RCf} \quad (3.32)$$

The duty cycle regulates output voltage of the BBC system. Therefore, employing the converter enables ones to produce outputs of any size. In addition, the output is zero whenever D is equal to 0, infinite if D is equal to 1, and proportional to the input if $D = 0.5$ (Abbasi & Mahjoob, 2013).

3.6 Mathematical Modelling of the system

The converter's state space mathematical model is produced by using a few fundamental operating principles. It is simple to compute the dynamics of this converter in CCM mode using Kirchhof's voltage and current law. The mentioned statement has been duly considered.

- The switch stays in the closed position for DT time interval and in the on position for (T-DT) time interval.
- The current flowing through the inductor remains continuous, meaning it is consistently positive.
- The circuit runs at steady state conditions.
- The capacitor is quite large, meaning that it should be larger than the minimum capacitance necessary for CCM in order to keep voltage overshoot to a minimum and keep the ripple voltage peak value under specific value.
- To maintain CCM and avoid much conduction losses in the switch and parasites resistances, inductor, inductor value should be bigger than the min inductor.

Figure 3.5 displays the Buck-Boost converter's fundamental schematic diagram. R_{in} , r_C , and r_L , respectively, stand for the input supply internal resistance, capacitor resistance and inductor resistance. We presume that the converter will function in CCM as a result of the element values.

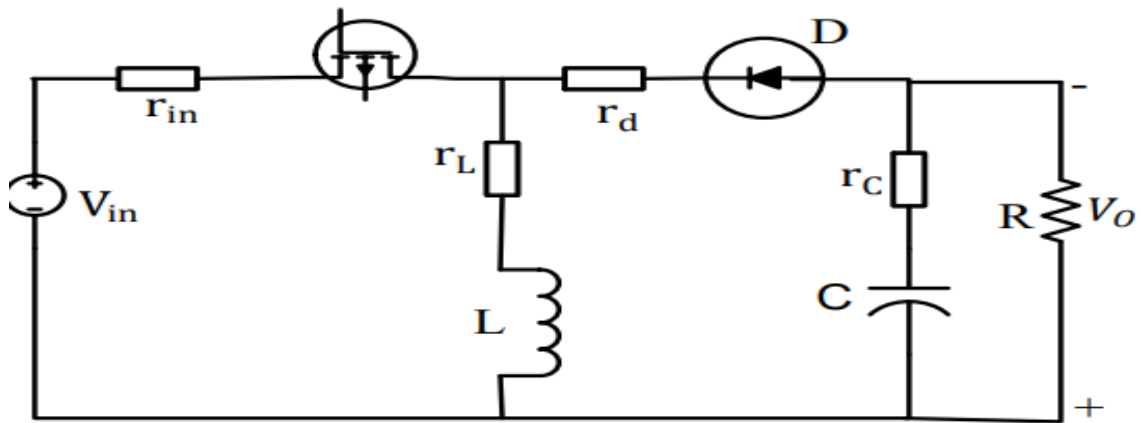
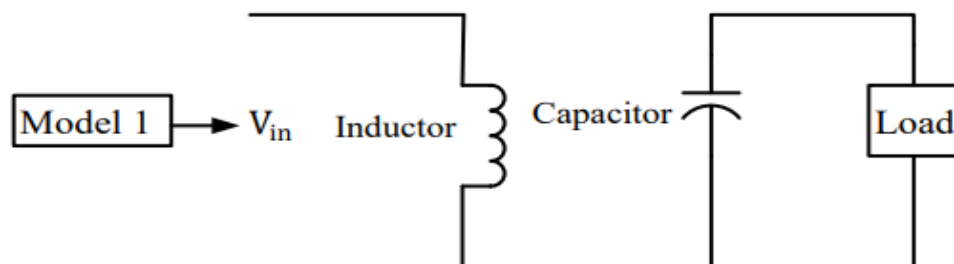


Figure 3.5 BBC circuit diagram

State space averaging is used during modelling. i_L is current flowing via the inductor and V_C is voltage along the capacitor, so the state vector is written as $\begin{bmatrix} i_L \\ V_C \end{bmatrix}$. The following continuous time state space equation serves as an example of the buck-boost converter.

$$\begin{cases} \dot{x}_1(t) = A_1 x(t) + B_1 V_s(t), & s = 0 \\ \dot{x}_2(t) = A_2 x(t) + B_2 V_s(t), & s = 1 \end{cases} \quad (3.33)$$

Here, $s = 1$ assign the on state of a switch whereas $s = 0$ assign the off state of a switch. Applying the double throw double pole switch using a passive diode D that is driven by the circuit's current and a firmly regulated MOSFET switch S that is always in the complimentary state. Only control signals are used to turn the switch S on or off. Figure 3.6 shows BBC's equivalent circuit.



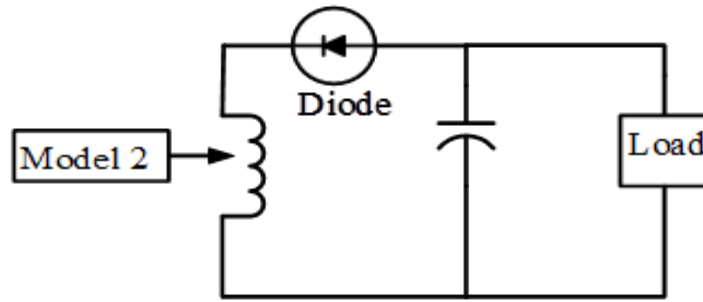


Figure 3.6 BBC equivalent circuit

Mode 1: As the switch is closed with reverse biased diode

As the diode is on the OFF state (reverse biased) and the load is unconnected to the input, while the transistor switch turned ON, the output voltage V_O becomes negative. Both the transistor and inductor allow the input current to pass through them. In Figure 3.7, it can be observed that MOSFETs are turned off when the gate pulses are high. This occurs periodically when the time lies within the range of $nT < t < nT + dT$, where n takes the values of 0, 1, 2, 3, and so on (Lewis, n.d.). The MOSFET remains turned off for dT seconds, as illustrated in Figure 3.7, which represents the equivalent circuit of the BBC in first mode.

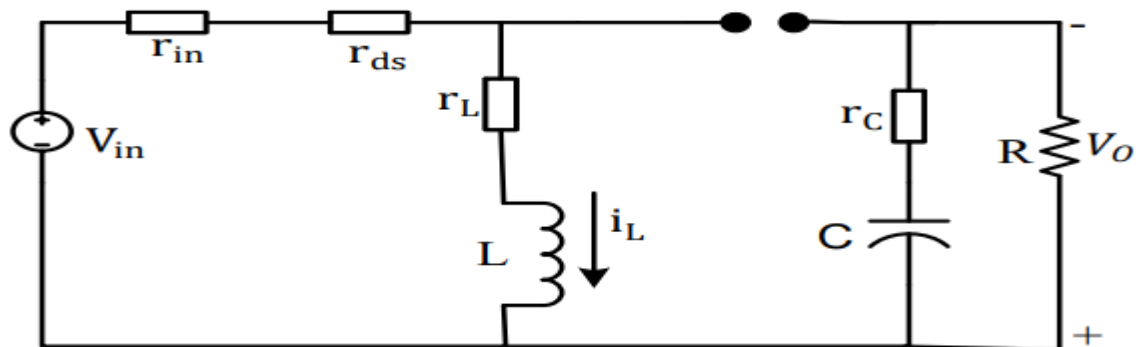


Figure 3.7 BBC as the switch is closed

Using Kirchof's current and voltage rule on the mode-1 circuit, the differential equations for state variables are as follows.

$$\begin{cases} V_i = i_L (r_i + r_{ds} + r_L) + L \frac{di_L}{dt} \\ r_C C \frac{dV_C}{dt} + V_C = -RC \frac{dV_C}{dt} \end{cases} \quad (3.34)$$

Then, using basic algebraic operations, constructing state equations by rearranging equation (3.34) and simplifying it.

$$\begin{cases} L \frac{di_L}{dt} = -i_L (r_i + r_L + r_{ds}) + V_i \\ C \frac{dV_C}{dt} = -\frac{V_C}{r_C + R} \end{cases} \quad (3.35)$$

The output equation V_O can be expressed as:

$$V_o = -\frac{RCdV_C}{dt} = \frac{RV_C}{r_C + R} \quad (3.36)$$

Equation (3.35) and (3.36) can be written as:

$$\begin{cases} \frac{dX(t)}{dt} = A_1X(t) + B_1U(t) \\ Y(t) = C_1X(t) + D_1U(t) \end{cases} \quad (3.37)$$

$$\text{Where, } A_1 = \begin{bmatrix} -\frac{1}{L}(r_i + r_L + r_{ds}) & 0 \\ 0 & -\frac{V_C}{(r_C + R)C} \end{bmatrix}, B_1 = \begin{bmatrix} 0 \\ \frac{1}{L} \end{bmatrix} \text{ and } C_1 = \begin{bmatrix} 0 & \frac{R}{R + r_C} \end{bmatrix}$$

State variables, namely $X(t)$, $U(t)$ and $Y(t)$, encompass different aspects of the converter's operation. Specifically, $X(t)$ denotes the output voltages and inductor current, $U(t)$ represents the input voltage to the BBC, and $Y(t)$ represents the output voltage.

Mode 2: As the switch is open with forward biased diode

In this mode, the switch is turned off based on control signal acted on it. As $i_L = \int \frac{V_L}{L} dt$, The diode is automatically switched on by the current flow i_L , eliminating the need for manual operation with control signals. It will be turned ON as the current passes to the left then turned off as the current passes to the right. On Figure 3.8, it can be observed that when the gate pulses are low, the MOSFETs open. This happens within the time range of $dT + nT < t < (nT + T) + dT$, where n takes the values of 0, 1, 2, 3, and so on, because of the periodic existing of the gate pulse. Consequently, the transistor remains open during $(1-d)T$ seconds. (Lewis, n.d.). The equivalent circuit of the BBC on second mode operation is seen below

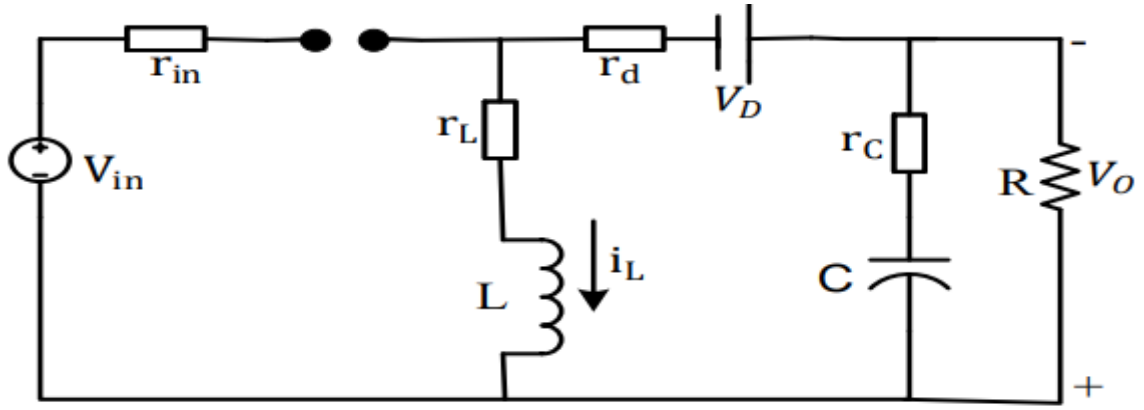


Figure 3.8 BBC as the switch is open

Kirchhof's current and voltage law is applied to the corresponding circuit for mode two:

$$\begin{cases} L \frac{di_L}{dt} + (r_d + r_L)i_L + V_D + r_C C \frac{dV_C}{dt} + V_C = 0 \\ r_C C \frac{dV_C}{dt} + V_C = R(i_L - C \frac{dV_C}{dt}) \end{cases} \quad (3.38)$$

Simple algebraic operations can be used to rearrange and simplify equations (3.38):

$$\begin{cases} L \frac{di_L}{dt} = -i_L (r_d + r_L) - V_D - r_C R \frac{di_L}{r_C + R} - \frac{V_C}{r_C + R} R \\ C \frac{dV_C}{dt} = \frac{Ri_L}{r_C + R} - \frac{V_C}{r_L + R} \end{cases} \quad (3.39)$$

The output V_O equation is as follows:

$$V_O = R(i_L - \frac{CdV_C}{dt}) = (\frac{r_C i_L}{r_C + R} + \frac{V_C}{r_C + R})R \quad (3.40)$$

$$\begin{cases} \frac{dX(t)}{dt} = A_2 X(t) + B_2 U(t) \\ Y(t) = C_2 X(t) + D_2 U(t) \end{cases} \quad (3.41)$$

where,
$$\begin{bmatrix} -\frac{1}{L} \left(r_d + r_L + r_C R \frac{1}{r_C + R} \right) & -\frac{R}{L(r_C + R)} \\ R \frac{1}{(r_C + R)C} & -\frac{1}{C(r_C + R)} \end{bmatrix}, \quad B_2 = \begin{bmatrix} 0 \\ 0 \end{bmatrix} \quad \text{and} \quad C_2 = \begin{bmatrix} \frac{Rr_C}{r_C + R} & \frac{1}{r_C + R} \end{bmatrix}$$

assume that $V_D = 0$

3.7 State-Space Average Model of the System

By taking the average of previously derived state equation over the switching cycle, state-space average model is produced. This is achieved by applying the duty cycle as multiplier and performing state-space averaging, thereby integrating the state equation to simple averaged equation. Considering that the transistor closes for a duration of dT sec and opens for $(T-dT)$ sec, so as to divide the resulting equation set by the averaged and valid period duration. The following equation represents the averaged equation for the inductor:

$$\begin{cases} L \frac{di_L}{dt} = -i_L (r_i + r_{ds} + r_L) + V_i, \text{ for } nT < t < (n+d)T \\ L \frac{di_L}{dt} = -i_L (r_d + r_L) - V_D - r_c R \frac{di_L}{r_c + R} - R \frac{V_C}{r_c + R}, \text{ for } (n+d)T < t < nT + T \end{cases} \quad (3.42)$$

The time interval's length is multiplied by the right and left sides of the equations.

$$\begin{cases} L \frac{di_L}{dt} \times dT = (-i_L (r_i + r_{ds} + r_L) + V_i) \times dT \\ L \frac{di_L}{dt} \times (1-d)T = (-i_L (r_d + r_L) - V_D - r_c R \frac{di_L}{r_c + R} - R \frac{V_C}{r_c + R}) \times (1-d)T \end{cases} \quad (3.43)$$

Averaging is accomplished by adding the corresponding sides together then multiply both side by reciprocal of T .

$$\begin{aligned} & L \frac{di_L}{dt} \times d + (1-d) \times L \frac{di_L}{dt} \\ & = d \times \left((-i_L (r_{ds} + r_L + r_i) + V_i) + (1-d) \times (-V_D - r_c R \frac{di_L}{r_c + R} - R \frac{V_C}{r_c + R} - (r_L + r_d)i_L) \right) \end{aligned} \quad (3.44)$$

Using a few fundamental algebraic procedures,

$$\begin{aligned} L \frac{di_L}{dt} & = d \times (- (r_{ds} + r_L + r_i) i_L) + dV_i \\ & + (1-d) \times \left(-i_L \left(r_d + r_L + r_c R \frac{1}{r_c + R} \right) \right) + \left(- \left(R \frac{V_C}{r_c + R} + V_D \right) \right) \times (1-d) \end{aligned} \quad (3.45)$$

Considering that:

$$R_1 = r_i + r_{ds} + r_L \quad (3.46)$$

$$R_2 = \frac{r_c}{r_c + R} + r_d + r_L \quad (3.47)$$

$$L \frac{di_L}{dt} = -d \times R_1 i_L + dV_i - R_2 i_L (1-d) - \frac{V_C}{r_c + R} R (1-d) - (1-d)V_D \quad (3.48)$$

The same method may be used to get the capacitor voltage equations:

$$\begin{cases} C \frac{dV_C}{dt} = -\frac{V_C}{r_c + R}, \text{ for } nT < t < (n+d)T \\ C \frac{dV_C}{dt} = R \frac{i_L}{r_c + R} - \frac{V_C}{r_c + R}, \text{ for } (n+d)T < t < nT + T \end{cases} \quad (3.49)$$

The time interval's length is multiplied by the right and left sides of the equations.

$$\begin{cases} C \frac{dV_C}{dt} \times dT = \left(-\frac{V_C}{r_c + R}\right) \times dT \\ C \frac{dV_C}{dt} \times (1-d)T = \left(R \frac{i_L}{r_c + R} - \frac{V_C}{r_c + R}\right) \times (1-d)T \end{cases} \quad (3.50)$$

The corresponding sides are joined together:

$$\begin{aligned} dT \times C \frac{dV_C}{dt} + (1-d)T \times C \frac{dV_C}{dt} &= dT \times \left(-\frac{V_C}{r_c + R}\right) \\ &+ (T-dT) \times \left(\frac{i_L}{r_c + R} R - \frac{V_C}{r_c + R}\right) \end{aligned} \quad (3.51)$$

Averaging is achieved by multiplying both sides by 1/T.

$$C \frac{dV_C}{dt} = d \times \left(-\frac{V_C}{r_c + R}\right) + (1-d) \times \left(R \frac{i_L}{r_c + R} - \frac{V_C}{r_c + R}\right) \quad (3.52)$$

Using a few fundamental algebraic procedures,

$$C \frac{dV_C}{dt} = R \frac{i_L}{r_c + R} \times (1-d) - \frac{V_C}{r_c + R} \quad (3.53)$$

The average system equation may so be written as,

$$\begin{cases} L \frac{di_L}{dt} = -dR_1 i_L + dV_i - (1-d)R_2 i_L - (1-d)R \frac{V_C}{r_c + R} - (1-d)V_D \\ C \frac{dV_C}{dt} = (1-d)R \frac{i_L}{r_c + R} - \frac{V_C}{r_c + R} \end{cases} \quad (3.54)$$

Where, $R_1 = r_i + r_L + r_{ds}$, and $R_2 = \frac{r_c}{r_c + R} + r_d + r_L$

Using the average system, it is possible to compute the steady-state voltages and currents. Zero must take the place of the left side in order to generate steady-state currents and voltages. Capital letters are used to indicate the steady state values. For instance, the symbol I_L stands for steady-state inductor current:

$$\begin{cases} 0 = -(DR_1 + R_2(1-D)) \times I_L - \frac{RV_C}{R+r_C}(1-D) - V_D(1-D) + DV_1 \\ 0 = R(1-D) \frac{I_L}{R+r_C} - \frac{V_C}{r_C+R} \end{cases} \quad (3.55)$$

So, the steady-state values are provided as:

$$\begin{cases} I_L = \frac{(r_C + R)(DV_1 - DV_D + V_D)}{RR_2 + R_2r_C - 2DR^2 + R^2 + D^2R^2 + DRR_1 - DRR_2 + DR_1r_C - DR_2r_C} \\ V_C = \frac{R(r_C + R)(D-1)(DV_1 - V_D + DV_D)}{RR_2 + R_2r_C - 2DR^2 + R^2 + D^2R^2 + DRR_1 - DRR_2 + DR_1r_C - DR_2r_C} \end{cases} \quad (3.56)$$

The averaging process also has to be employed for the output equation:

$$\begin{cases} V_o \times dT = \frac{V_C}{R+r_C} R \times dT \\ V_o \times (T-dT) = R \left(r_C \frac{i_L}{R+r_C} + \frac{V_C}{R+r_C} \right) \times (T-dT) \end{cases} \quad (3.57)$$

The corresponding sides are joined together:

$$V_o \times d.T + V_o \times (1-d).T = R \frac{V_C}{r_C+R} \times d.T + \left(r_C \frac{i_L}{r_C+R} + \frac{V_C}{r_C+R} \right) R \times (T-dT) \quad (3.58)$$

The equation set is averaged after multiply both sides by $1/T$. The result of applying the fundamental algebraic operations and then multiplying both side by reciprocal of T is:

$$V_o = (1-d)R \frac{r_C i_L}{r_C+R} + R \frac{V_C}{r_C+R} \quad (3.59)$$

Since the control parameter (d) is incorporated into matrix A , state-space average model for the BBC with the load R exhibits a non-linear characteristic.

3.8 Impact of Parasitic Components on the System Performance

Capacitor, inductor and MOSFET switch are utilized in the converters. These all have parasitic components that compromise the BBC's efficiency. Limiting the duty ratio prevents the voltage gain from decreasing due to parasitic components. Gain increases because to the parasitic element up to a specific duty ratio value, beyond which gain significantly decreases. Figure 3.9 shows BBC's circuit with impact of parasitic elements.

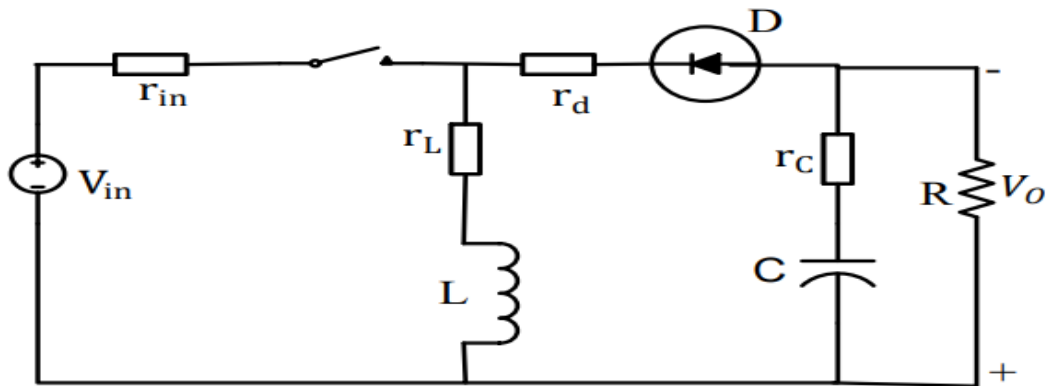


Figure 3.9 BBC circuit with impact of parasitic elements

Parasitic component's impact in MOSFET:

As the MOSFET becomes reverse biased, an internal diode that is linked in parallel with it illuminates. Reverse voltage protection is supplied by this internal diode. The model is created using an ideal switch, and a gate signal (g) is used to toggle it ON or OFF. The switch and diode are linked in parallel. Figure 3.10 shows the MOSFET with its equivalent circuit.

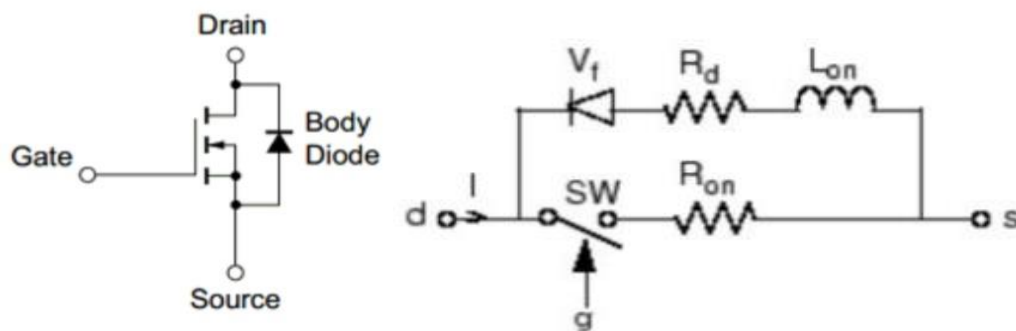


Figure 3.10 MOSFET with its equivalent circuit

The following factors will affect how a MOSFET's ON state voltage, V_{ds} , varies:

- ✓ As it is turned ON, the voltage across the drain and source (V_{ds}) is equivalent to the product of the on-state resistance ($R_{ds(on)}$) and the current (I) flowing through the component at that particular moment.
- ✓ Conversely, as it is switched OFF, the anti-parallel diode begins to conduct.

V_f is the internal diode forward voltage drops, and $V_{ds} = R_d I - V_f + L_{on}(di/dt)$. Only continuous systems employ the antiparallel diode inductance, abbreviated L_{on} . This value is 0 for discrete systems.

3.9 Stability Analysis

3.9.1 Equilibrium Points

Considering the non-linear state-space model provided as:

$$\dot{x}(t) = f(t, x(t)), \text{ for } t \geq 0$$

Equilibrium is said to exist for a vector x_0 if:

$$f(t, x_0) = 0, \text{ for } \forall t \geq 0$$

The differential equation's equilibrium points are its solutions, and each solution point establishes an equilibrium point (G. V. Mohammed Dahleh, n.d.)

Using the buck-boost state space equation, we can derive:

$$\begin{cases} \dot{x}_1 = \frac{(d-1)}{L} x_2 + \frac{d}{L} u(t) \\ \dot{x}_2 = -\frac{1}{RC} x_2 + (d-1) \frac{-1}{C} x_1 \end{cases} \quad (3.60)$$

where x_2 denotes the converter output voltage and x_1 its output inductor current. Once more using equation (3.60), let f_1 and f_2 be f_1 and f_2 , respectively. = 0

$$\begin{cases} \frac{(d-1)}{L} x_2 + \frac{d}{L} u(t) = 0 & \text{(i)} \\ -\frac{1}{RC} x_2 + (d-1) \frac{-1}{C} x_1 = 0 & \text{(ii)} \end{cases} \quad (3.61)$$

Solving for x_2 using equation (3.61) of (i):

$$x_2 = -\frac{d}{(d-1)}u(t) \quad (3.62)$$

Equation (3.62) is plugged into equation (3.61) of (ii), which is then solved for x_1 :

$$x_1 = -\frac{d}{R(d-1)^2}u(t) \quad (3.63)$$

As a result, the equilibrium points are listed here below:

$$\begin{cases} x_1 = -\frac{d}{R(d-1)^2}u(t) \\ x_2 = -\frac{d}{(d-1)}u(t) \end{cases} \quad (3.64)$$

It can be seen from equation (3.64) that the converter's equilibrium point depends on input and shows a bifurcation behaviour. We may obtain the values of x_1 and x_2 by substituting the parameter values from appendix A, i.e., $x_1 = 5.25$ and $x_2 = 24.46$.

3.9.2 Checking stability of non-linear system

The equilibrium points serve as the basis for defining stability in nonlinear systems. If the solution beginning from the initial state within the ball with a tiny radius stays inside that ball for whole time, then the equilibrium point is stable. If an equilibrium point is unstable, it could be because of any of the following factors (G. V. Mohammed Dahleh, n.d.).

- From an initial condition, the system trajectory extends to infinity.
- The solution trajectory deviates greatly from the equilibrium location.
- A limit cycle is formed by the system's trajectory.

3.9.3 Local stability analysis

When employing the Lyapunov/direct technique to examine local stability, two essential steps are followed.

Step-1: Selecting a definite positive Lyapunov function is the first step.

Definition: Suppose we have a Lyapunov function, denoted as V , which is a continuous mapping from R^n (n-dimensional Euclidean space) to the real numbers (R). We say that $V(x)$ is a function locally positive definite around $x = x_0$ if:

- i. $V(x_0) = 0$
- ii. $V(x) > 0, 0 < \|x\| < r$ (G. V. Mohammed Dahleh, n.d.).

Step-2: Following that, the second step is analysing the derivative of the Lyapunov function along state trajectory towards the equilibrium point.

Theorem: - If a system possesses a Lyapunov function $V(x)$, then a point $x = x_0$ is considered a Lyapunov point if, in addition, the derivative of the Lyapunov function $V(x_0)$ is greater than zero for all x within a certain radius $0 < \|x\| < r$. In such cases, the point $x = x_0$ is asymptotically stable equilibrium point. (G. V. Mohammed Dahleh, n.d.).

By selecting the Lyapunov function, positive definite function $V = \frac{1}{2}x_1^2 + \frac{1}{2}x_2^2$, calculating the derivative of Lyapunov function, $\dot{V} = x_1\dot{x}_1 + x_2\dot{x}_2$, and determining \dot{V} around the equilibrium point $\dot{V} < 0$, the stability of the BBC equilibrium points is checked. As a result, the equilibrium points in the x direction behave consistently.

The states ($x=x_1, x_2$, and $y=x_1, x_2$) start at $[0, 0.01]$ and move away to $[40, 20]$ after ten seconds. The beginning position $[24.46, 5.25]$ is distant from equilibrium point, but after ten seconds it either remains near equilibrium point or advances to equilibrium point from the original conditions. This suggests that equilibrium point displays steady behaviour.

3.10 System Controller Design

3.10.1 Sliding mode control

SMC is considered as a reliable control mechanism for complex higher order nonlinear systems where external disturbances and parametric uncertainties are present. In the 1950s in the former Soviet Union, SMC operation was initially developed in variable structure systems (Alam et al., 2018). The variable structure system was not able to give focus throughout the early design phase of the project. mostly due to chattering problems with sensors, actuators, and switching methods, and the complexity of the execution. However, this strategy has some significant benefits as it modifies the system's dynamic behaviour by selecting the proper switching function, rendering the closed loop result non-sensitive to matched uncertainty in the system. Recently, SMC design methods have been used to address important problems including reducing chattering, compensating for the effects of unstructured dynamic, adapting to uncertain system, and advancing the dynamic performance of closed loop systems. The main merit of using an SMC over a linear controller like PID is that SMC offers stability and resilience performance in a variety of uncertain system, whereas PID is incapable in the presence of uncertainty. SMC is a reliable nonlinear control method with strong disturbance rejection and plant uncertainty capabilities. This

control strategy operates on the tenet of continually changing the controller's configuration to keep the state variables along the sliding surface. Figure 3.11 shows phase portrait of sliding motion in SMC (Gambhire et al., 2021) (Alam et al., 2018).

The two distinct steps of SMC synthesis are the design of sliding surface and design of control input. It has been determined that building the sliding surface, which is anticipated to give response to the specified control needs and performances, is the most important phase in constructing the SMC. As seen in the figure below (Ghazali et al., 2011) the state trajectories are compelled to reach and stays on the sliding surface.

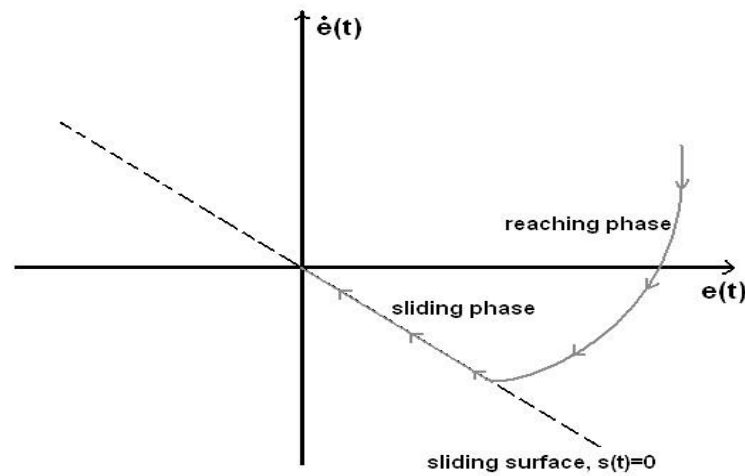


Figure 3.11 Phase portrait of sliding motion in SMC

In an SMC architecture, the control signal consists of switching and comparable controls, with the control action matching to the sliding phase and reaching phase.

The sliding surfaces should be chosen before designing the SMC. The surface might comprise elements like PD, PI, and PID.

It could be think of the scalar discontinuous control action $u=u(s,t)$ at time t as common Sliding Mode Theory (Utkin, 1992).

$$u(s, t) = -K(t) \text{sign}(s) \tag{3.65}$$

$$\text{sign}(s) := \begin{cases} 1 & \text{if } s > 0 \\ -1 & \text{if } s < 0 \\ 0 & \text{if } s = 0 \end{cases} \tag{3.66}$$

3.10.2 Design of super twisting sliding mode controller

As previously indicated, chattering is the fundamental weakness of first-order sliding mode control (FOSMC). The system variables' oscillation around the sliding surface, that results in discontinuous control signal, is what creates this phenomenon. The physical system may be disturbed or harmed by this impact. Utilizing HOSM is one of the intriguing methods to get rid of or minimize the chattering impact. The higher order time derivative of the sliding surface remain zero in such method (Shtessel et al., 2014). This operation thereby reduces the chattering impact. but, the basic issue in implementing HOSM algorithm is the rising information demand. The (r-1)-th order of time derivative is often necessary for an r-th order sliding controller. Consequently, this order of sliding mode is constructed by

$$s = \dot{s} = \ddot{s} = \dots = s^{(r-1)} = 0 \quad (3.67)$$

Consequently, the second-order SMC is straightforward. Actually, it is necessary to understand the sliding surface's first-order time derivative. Real time measuring of \dot{s} or in the very least of $\text{sign}(\dot{s})$ is necessary for these controllers.

The super-twisting controller, among other second-order sliding mode controllers, has the advantage of not needing any prior knowledge of \dot{s} . Having the same data, the first-order (standard) sliding mode may be replaced by the super-twisting controller. The trajectory of ST controller is seen in Figure 3.12 (Nasiri et al., 2019).

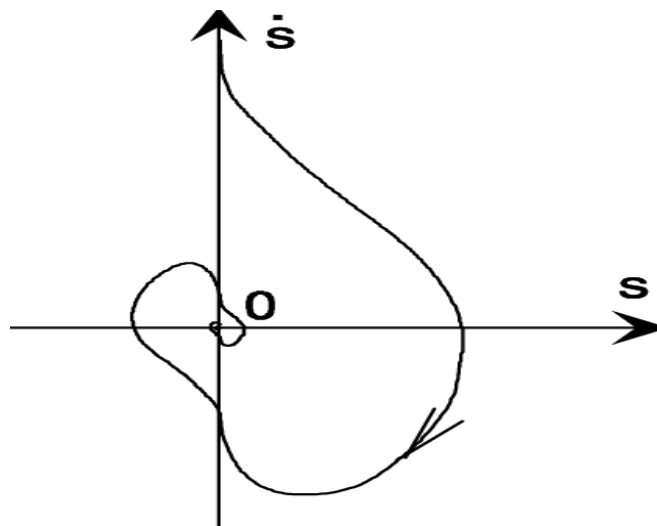


Figure 3.12 Trajectory of super-twisting controller.

For this system controller design choosing such surface comprising of both current and voltage states that mean choosing PI surface for voltage and steady state equation for current state as:

$$\left. \begin{aligned} S_1 &= C_1 e_1 \\ S_2 &= C_2 e_2 + C_3 \int e_2 dt \end{aligned} \right\}, S = S_1 + S_2 \quad (3.68)$$

Where C_1 , C_2 and C_3 are a sliding constants and then e_1 and e_2 are current and voltage error respectively.

Now consider the state-space model for BBC at steady state.

$$\left\{ \begin{aligned} \frac{(d-1)}{L} x_2 + \frac{d}{L} u(t) &= 0 & (i) \\ -\frac{1}{RC} x_2 + (d-1) \frac{-1}{C} x_1 &= 0 & (ii) \end{aligned} \right. \quad (3.69)$$

Solving for d using Equation (3.69) of (i):

$$d = \frac{x_2}{x_2 + u(t)} \quad (3.70)$$

Solving for x_1 using Equation (3.69) of (ii):

$$x_1 = \frac{x_2}{R(1-d)} \quad (3.71)$$

Equation (3.70) is plugged in to Equation (3.71), which is then solved for x_1 :

$$x_1 = \frac{x_2}{Ru(t)} (x_2 + u(t)) \quad (3.72)$$

Now at steady state, Equation (3.72) can be stated as

$$i_d = \frac{V_d}{Rv_i} (v_d + v_i) \quad (3.73)$$

Where i_d is the desired inductor current and v_d is the desired voltage with given input voltage $u(t)=v_i$.

Now, it is to define the current and voltage errors. The error could be determined as a difference between the desired and actual output.

$$\begin{cases} e_1 = i_d - x_1 \\ \dot{e}_1 = -\dot{x}_1 \end{cases} \quad (3.74)$$

$$\begin{cases} e_2 = v_d - x_2 \\ \dot{e}_2 = -\dot{x}_2 \end{cases} \quad (3.75)$$

In sliding phase, the error will converge to equilibrium point and the sliding surface is expected to be $s(t) = \dot{s}(t) = \ddot{s}(t) = 0$ where in such situation, the error is captured in the surface. The equivalent control is produced as $\ddot{s}(t) = 0$.

Differentiating the sliding surface S_1 of Equation (3.68) as follow

$$\left. \begin{aligned} \dot{S}_1 &= C_1 \dot{e}_1 \\ \dot{S}_2 &= C_2 \dot{e}_2 + C_3 e_2 \end{aligned} \right\}, \dot{S} = \dot{S}_1 + \dot{S}_2 \quad (3.76)$$

Inserting Equation (3.74) and (3.75) in Equation (3.76)

$$\dot{S} = C_1 \dot{e}_1 + C_2 \dot{e}_2 + C_3 e_2 \quad (3.77)$$

$$\dot{S} = C_1 \dot{x}_1 + C_2 (-\dot{x}_2) + C_3 (v_d - x_2) \quad (3.78)$$

From the state-space model of BBC, inserting Equation (3.60) into Equation (3.78).

$$\dot{S} = C_1 \left(\frac{(d-1)}{L} x_2 + \frac{d}{L} v_i \right) + C_2 \left(-\left(-\frac{1}{RC} x_2 + (d-1) \frac{-1}{C} x_1 \right) \right) + C_3 (v_d - x_2) \quad (3.79)$$

The Lyapunov theorem is the well-known method that is used in stability research to confirm the convergence behaviour of non-linear controllers (Hu et al., 2022);(Wu et al., 2019);(Dai et al., 2019).The Lyapunov function, whose time derivative is provided in Equation (3.78), can be used to demonstrate stability as in Equation (3.77).

$$V = \frac{1}{2} s^2 \quad (3.80)$$

$$\dot{V} = s\dot{s} \quad (3.81)$$

For $s \neq 0$, $V = 0$ and $V > 0$. Following the reaching condition is important to ensure that the transitions of trajectory from reaching phase to sliding phase and maintains stability.

$$\dot{V} < 0, \text{ for } s \neq 0, \dot{s} \neq 0 \quad (3.82)$$

For $S_1 \dot{S}_1 \leq 0$, Equation (3.79) becomes

$$C_1\left(\frac{(d-1)}{L}x_2 + \frac{d}{L}v_i\right) + C_2\left(-\left(-\frac{1}{RC}x_2 + (d-1)\frac{-1}{C}x_1\right)\right) + C_3(v_d - x_2) = 0 \quad (3.83)$$

Taking the duty cycle d as a control signal u (i.e., $u=d$)

$$\begin{cases} C_1\left(\frac{(d-1)}{L}x_2 + \frac{d}{L}v_i\right) + C_2\left(-\left(-\frac{1}{RC}x_2 + (d-1)\frac{-1}{C}x_1\right)\right) + C_3(v_d - x_2) = 0 \\ C_1\left(\frac{(u-1)}{L}x_2 + \frac{u}{L}v_i\right) + C_2\left(-\left(-\frac{1}{RC}x_2 + (u-1)\frac{-1}{C}x_1\right)\right) + C_3(v_d - x_2) = 0 \end{cases} \quad (3.84)$$

Rearranging for u ,

$$u\left(\frac{C_1}{L}x_2 + \frac{C_1}{L}v_i + \frac{C_2}{C}x_1\right) = \frac{C_1}{L}x_2 - \frac{C_2}{RC}x_2 + C_3x_2 + \frac{C_2}{C}x_1 + C_3v_d \quad (3.85)$$

Now multiply both side of equation (3.85) by LC and then solve for u

$$u(C_1Cx_2 + C_1Cv_i + C_2Lx_1) = C_1Cx_2 - \frac{C_2L}{R}x_2 + C_3LCx_2 + C_2Lx_1 + C_3LCv_d \quad (3.86)$$

Therefore, the equivalent controller is simplified as (i.e., $u_{eq}=u$),

$$u_{eq} = \frac{\left(C_1C - \frac{C_2L}{R} + C_3LC\right)x_2 + C_2Lx_1 + C_3LCv_d}{C_1C(x_2 + v_i) + C_2Lx_1} \quad (3.87)$$

The control law u in SMC combines two different forms of control provided by:

$$U = u_{eq} + u_c \quad (3.88)$$

Where u_{eq} is the equivalent controller employed in controlling the system state while the sliding surface is in motion. For the equivalent control, we utilize equation (3.85). using the control action input provided for STSMC by (Ouchen et al., 2021); (Humaidi & Hasan, 2019); (Zhao et al., 2018):

$$u_c = -K_1\sqrt{|s|}\text{sgn}(s) - K_2 \int_0^t \text{sgn}(s)dt \quad (3.89)$$

In order to control voltage for BBC system, the STSMC controller was designed as follows:

Inserting Equation (3.87) and Equation (3.89) in Equation (3.88), it become,

$$U = \frac{\left(C_1C - \frac{C_2L}{R} + C_3LC\right)x_2 + C_2Lx_1 + C_3LCv_d}{C_1C(x_2 + v_i) + C_2Lx_1} + \left(-K_1\sqrt{|s|}\text{sgn}(s) - K_2 \int_0^t \text{sgn}(s)dt\right) \quad (3.90)$$

Where C_1 , C_2 , C_3 , K_1 and K_2 are constant gain parameters.

3.10.3 PID controller for the System

Significant advancements have been made in process automation technology since the 1980s. Particularly controller processing power has risen significantly, which has an impact on the kinds of controls used in applications. In the past, the majority of controllers used a single loop and a single variable. Multiple applications now often use multiloop and multivariable controllers (Hussein et al., 2015). These control strategies are built on the PID controller. This system consists of a proportional element, derivative element, and integral element. The PID controller becomes inefficient when there are changes in the external environment because the gain constants are set initially and remain constant throughout the operation. Figure 3.13 shows the block diagram for PID controller of any system, where all PID components are interconnected in parallel. The proportional (P), integral (I), and derivative (D) gains are represented by K_p , K_i , and K_d , respectively. The error sigma serves as the input to the controller.

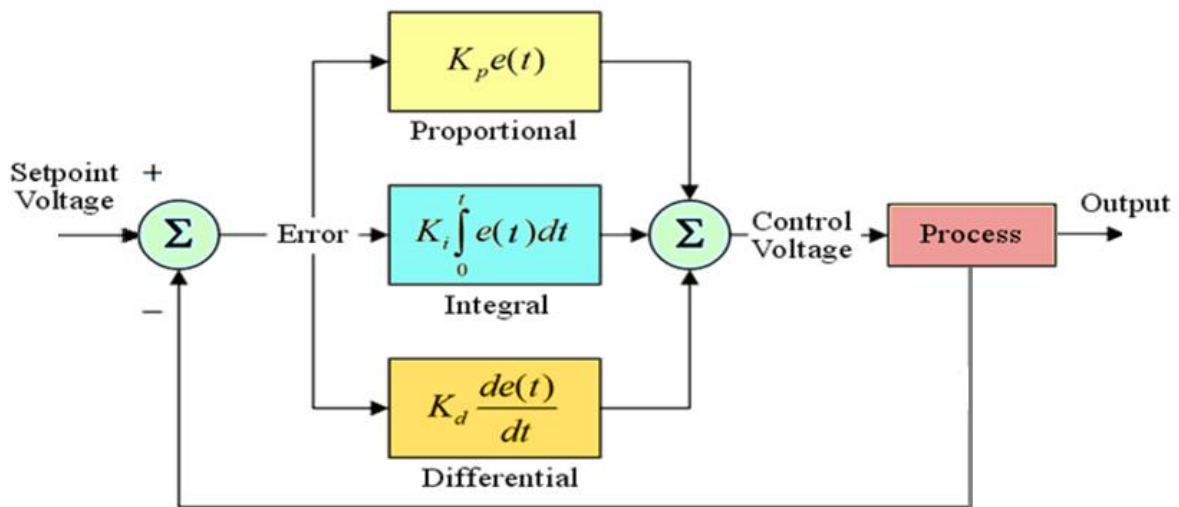


Figure 3.13 Block Diagram of PID Controller (Hussein et al., 2015)

The output of PID controller is as follows:

$$U(t) = K_p e(t) + K_i \int_0^t e(t) dt + \frac{K_d de(t)}{dt} \quad (3.91)$$

In this context, K_p , K_i , and K_d represent proportional, integral, and derivative gain, respectively.

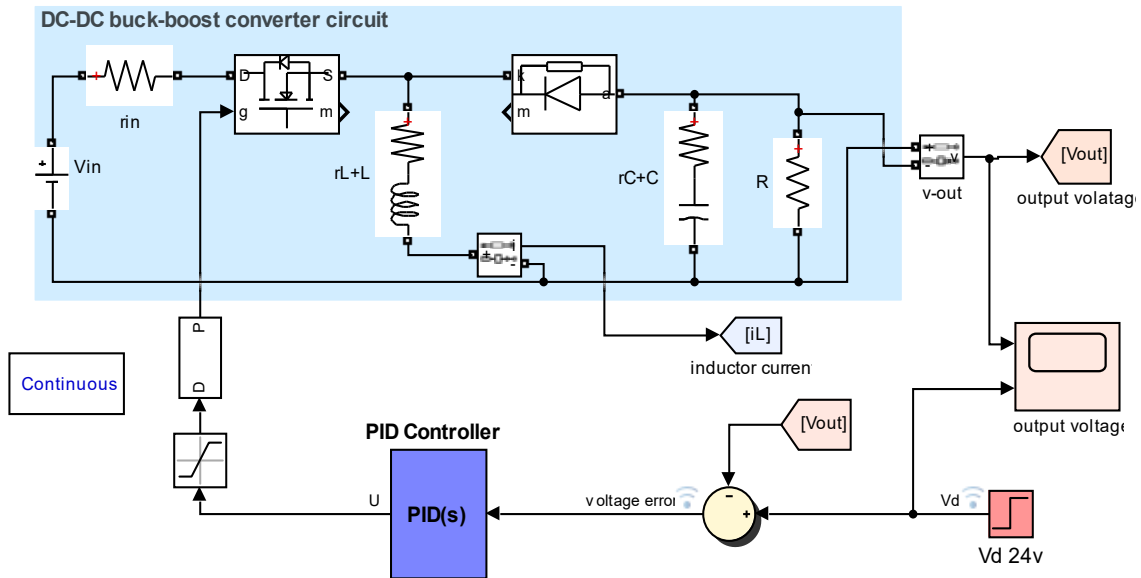


Figure 3.14 The PID controller for DC-DC Buck-Boost converter

The block diagram of a BBC with PID controller is depicted in Figure 3.14. The duration for that the switch is toggled on each switching cycle is controlled by input signal, which enters the pulse width modulation. The limiter included in the circuit of the buck-boost converter defines the theoretical range within which the magnitude of the control signal can be adjusted from zero to one. This limitation brings about a new nonlinearity that wasn't taken into consideration while developing the model of BBC system.

3.10.4 The Proposed Methods of Optimization

One criterion in the design of resilient controllers is the selection of appropriate optimization techniques. The methods used for optimizing the controllers gain that are particle swarm optimization and genetic algorithm, are briefly discussed in the section that follows.

3.10.5 Genetic Algorithms (GA)

The Genetic Algorithm (GA) is a method that utilizes principles of genetic selection to optimize search algorithms for complex problems. It finds applications not only in optimization but also in machine learning, research, and development. By combining elements such as selection, crossover, and mutation, which mimic genetic operations found in natural populations, GA resembles biological processes of chromosome formation.

The primary objective of GA is to generate improved solutions for successive generations. In the context of graph problems, the use of path encoding enables GA to identify shorter paths by representing them as chromosomes. The success of individual solutions is closely

tioned to their fitness, which determines their likelihood of producing offspring and contributes to the overall quality improvement in subsequent generations.

Once it is determined that a GA is the most suitable approach for tackling optimization challenges in a computational system, the procedure is considered complete. The credit for developing the first genetic algorithm goes to John Holland, and the algorithm gained prominence in the 1970s as its funding decade. This approach is chosen to effectively address complex problems, Charles Darwin also proposed a random search strategy for a specified search space (Lambora et al., 2019); (S. Mirjalili, J. Song Dong, A. S. Sadiq, 2020).

A "population" of potential solutions to the issue are generated by the algorithm, and they are given the freedom to reproduce over time to produce better ones. When the population reaches an acceptable level of fitness or a predetermined number of generations have been created, the algorithm is finished. A good solution may or may not have been discovered if the approach ran out of generations allowed (Farahmandrad et al., 2020).

3.10.6 Particle Swarm Optimization

Particle swarm optimization (PSO) is an efficient method for solving non-linear, multi-dimensional problems with minimal parameterization. It is capable of achieving excellent results in terms of optimization while minimizing the need for adjusting numerous parameters. (Clerc, 2010).

Nature has always been a tremendous source of inspiration for research throughout time, and there is always plenty to learn and discover about it. The goal of Swarm Intelligence (SI), a significant subfield of artificial intelligence, is for simulating the group behaviour of social swarming in nature. Undoubtedly one of the most well-liked SI paradigms is the Particle Swarm Optimization algorithm (PSO). PSO has gained prominence in the optimization sector over the past 20 years by being effectively utilized, with good results as well, in a wide range of scientific and technology fields with a greater range of complicated optimization issues. However, further research has shown a number of flaws with the method, including concerns with convergence, diversity, and stability. As a result, notably following the turn of the twentieth century, PSO has seen a wide range of improvements, expansions, and modifications in many elements of the algorithm, and the associated research has therefore now achieved an amazing level. PSO was first developed in the middle of the 1990s. Swarm algorithms are being utilized more often in a variety of sectors to optimize various sorts of issues.

These algorithms may frequently handle challenging optimization issues with simple implementation and few technical presumptions. For instance, having a differentiable or separable objective function is not necessary. These algorithms' adaptability gives them the potential to address a variety of real-world optimization cases in a variety of fields, including engineering and computer science (Houssein et al., 2021).

3.10.7 Objective Functions

A performance index needs to be designed in order to achieve the desired dynamic and steady state features while preventing excessive controller output. The most crucial stage in applying any optimization approach is choosing the objective functions that will be applied to evaluate the fitness (or particle) of each population. The cost function that minimizes the system inaccuracy is objective cost functions (Al-Mayyahi et al., 2016), which is set as:

$$ITAE = \int_0^{\tau} t(|e(t)|)d\tau \quad (3.92)$$

here, $e(t)$ is error b/n the reference and output voltage.

3.10.8 GA based PID controller

Genetic algorithms are a computational approach inspired by the process of natural selection and evolution. They are used to solve optimization and search problems by mimicking the principles of biological evolution. It is an adaptive approach used to address search and optimization challenges, specifically to fine-tune controller settings in order to achieve the desired transient response without compromising steady-state operation. Figure 3.15 shows the structure of the GA-PID Controller.

GA-Proportional Integral Derivative (PID) Controller Structure

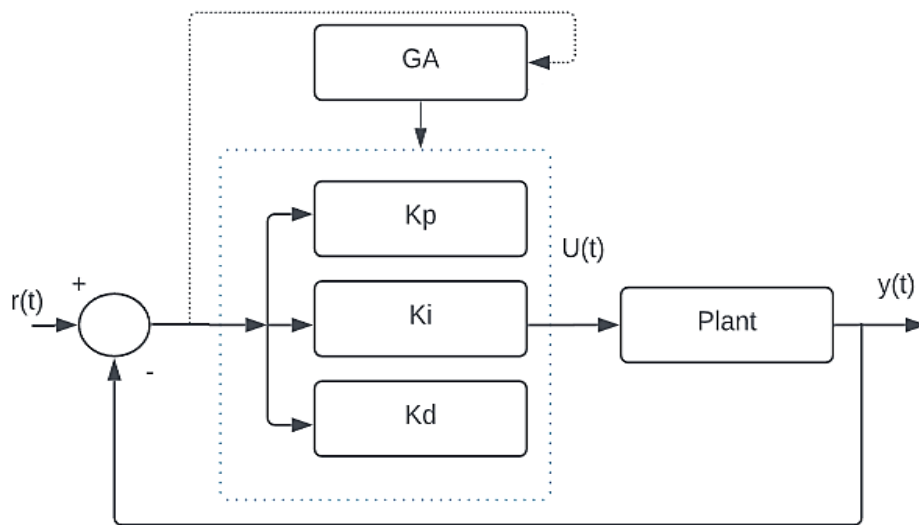


Figure 3.15 Structure of the GA-PID Controller

The concept and implementation of the GA-PID controller are described in this section. These are the actions in the following order:

Step-1: Establishing an initial population of solutions for the parameters K_p , K_i , and K_d .

Step-2: Evaluating fitness function

The quality or effectiveness of a solution is evaluated by assigning it a numerical value, which is achieved through the use of an appropriate fitness function tailored to the specific problem. The fitness function outlined below serves this purpose. (Conference, 2012):

Step 3: Generating offspring

Mutation, Crossover and selection are involved.

Step 4: Replacing existing population by new population

Step 5: Terminating the program as if termination existed, or back to the second step.

The implementation of the GA-PID controller for the BBC. below illustrates the specifics of the GA parameter settings for adjusting the PID controller.

- Number of Generations: 20
- Number of Population: 30
- Lower Bound (LB): [0.001 10 1e-08]
- Upper Bound (UB): [0.004 40 1e-07]

Figure 3.16 depicts the convergence curves for the mean and best fitness values for GA.

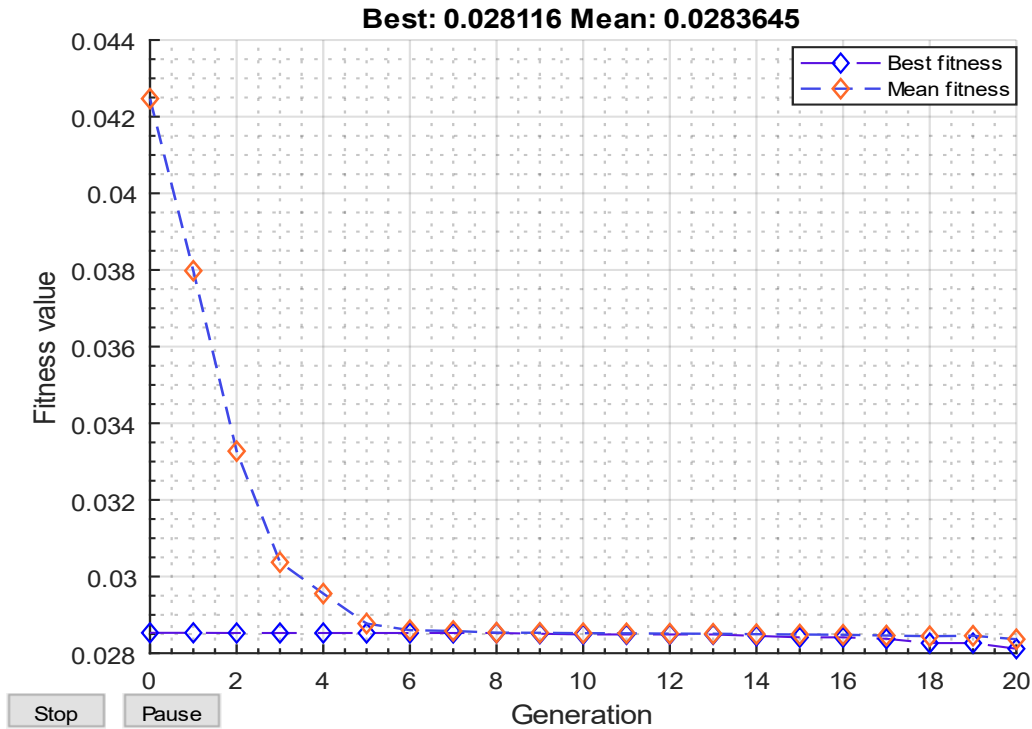


Figure 3.16 The convergence characteristic curve.

GA optimization is used to simulate a BBC system for PID voltage control. The converter's parameters for controlling voltage under GA-PID controller gain as $K_p=0.00146$, $K_i=35.8691$ and, $K_d=3.241e-08$ are derived. The performance of such controlling method is covered in the next chapter. Using the described procedures, a GA based PID controller is applied on a buck-boost for controlling voltages.

3.11 Overall System Structure

The overall system structure of the proposed system is depicted in Figure 3.17.

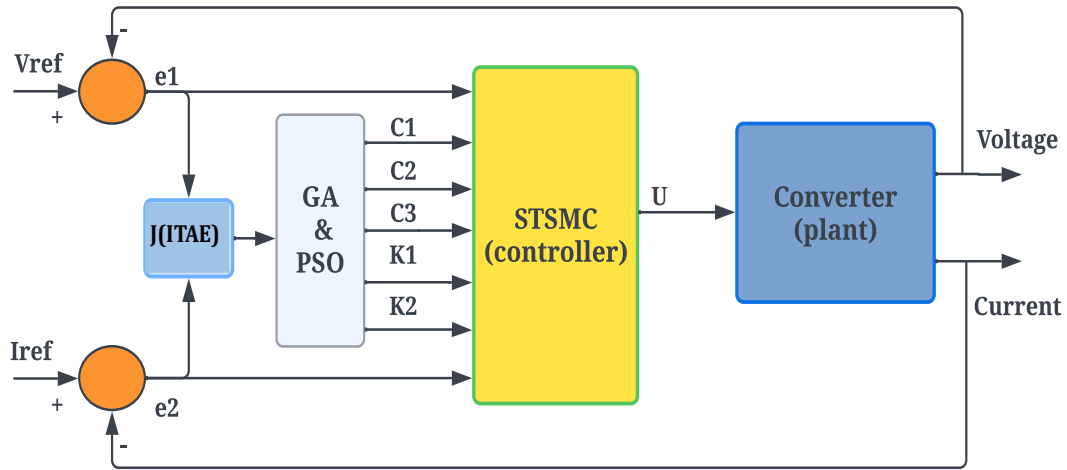


Figure 3.17 Overall system structure

PSO and GA are used to fine-tune the settings of the STSMC controller in order to manage the voltage of the BBC. It is possible to make comparison which tuning method is best for such specific application by tuning the parameters of controllers using these two ways. In terms of fitness value, computing time, and other factors, this algorithm is compared. The convergent curve of this two-optimization procedure is depicted in Figure 3.18 and 3.19 below. The tuning parameters and boundary values are specified in the Table 3.1

Table 3:1 Boundaries for tuning parameters of controller.

Boundaries	STSMC				
	C1	C2	C3	K1	K2
Lower Bound (LB)	0.001	-20	-20	0	0
Upper Bound (UB)	20	15	15	10	10

The control's parameters are adjusted in relation to the suggested cost function (J) using the PSO and GA. The tuning settings for the parameters are established as seen in Table 3.2.

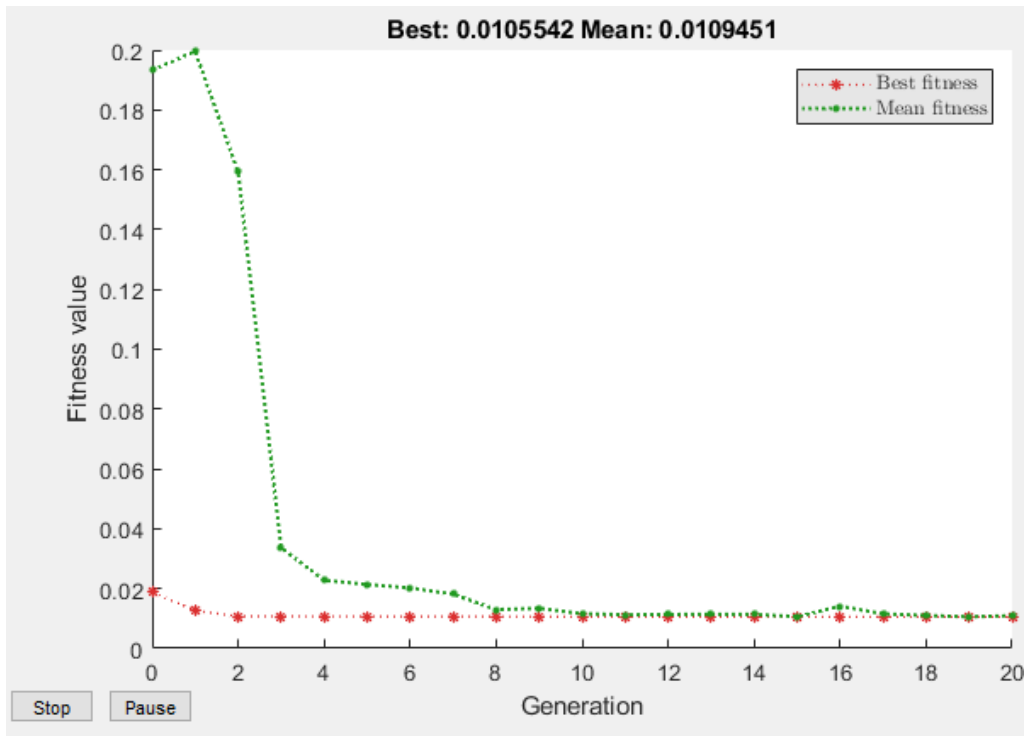


Figure 3.18 Convergent curve for GA

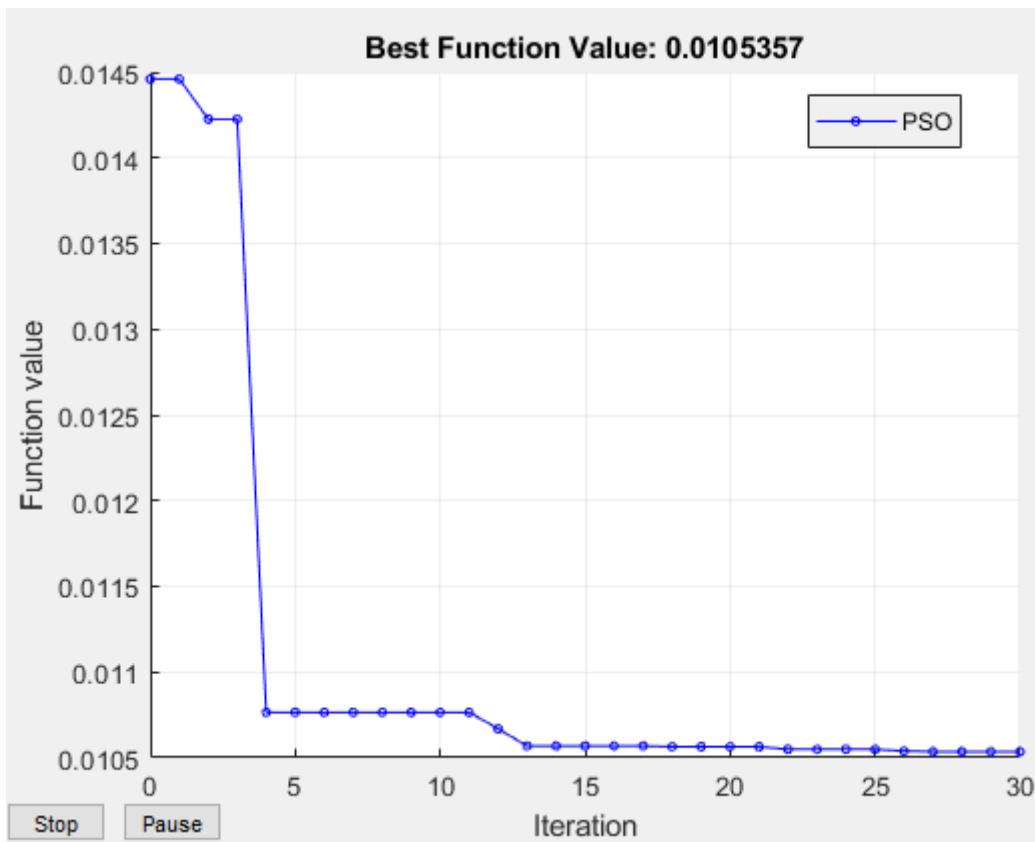


Figure 3.19 Convergent curve for PSO

Table 3:2 Parameters for the algorithms.

Algorithm	Parameters	
PSO	Number of Particles	20
	Maximum Iteration	30
GA	Population size	20
	Generation	20

The proposed algorithms were applied on the STSMC controller. First, coding is used to export PSO and GA to the MATLAB. The proposed algorithms are run for 30 iterations (PSO) and 20 generation (GA) to obtain the cost function's (J) minimum value. The optimal STSMC parameter values after tuning are shown in Table 3.3, correlating to the min cost function values delivered by the GA and PSO. Additionally, Table 3.3 shows the amount of the min cost function (Jmin).

Table 3:3 The proposed STSMC's Optimal values.

Controller parameters		PSO	GA
STSMC	C1	18.1012	12.0151
	C2	-10.1321	-10.1033
	C3	-9.0215	-8.2031
	K1	0.08360	0.08358
	K2	0.1064	0.1059
Best value (Jmin)		0.0105357	0.0105542

The PSO outperforms GA in terms of best value. The amount of time required for tuning rely on the window, the CPU, the MATLAB version, the step-time, and other factors. Therefore, the processor in this work window is 3.19 GHz, the MATLAB version is R2019b.

CHAPTER FOUR

RESULT AND DISCUSSION

4.1 Introduction

The proposed super twisting sliding mode controller system of the DC-DC buck-boost converter's result and analysis are included in this chapter. To achieve the specified goals of the research, the simulation outcomes of the BBC system was compared with that of PID controller. The converter's parameters from Table 4.1 were used to run the simulation. The voltage, and subsequently the current, are controlled by STSMC. In order to create good system performance, controller's parameters are optimized using GA and PSO. Figure 4.1 depicts how the MATLAB/Simulink BBC is designed.

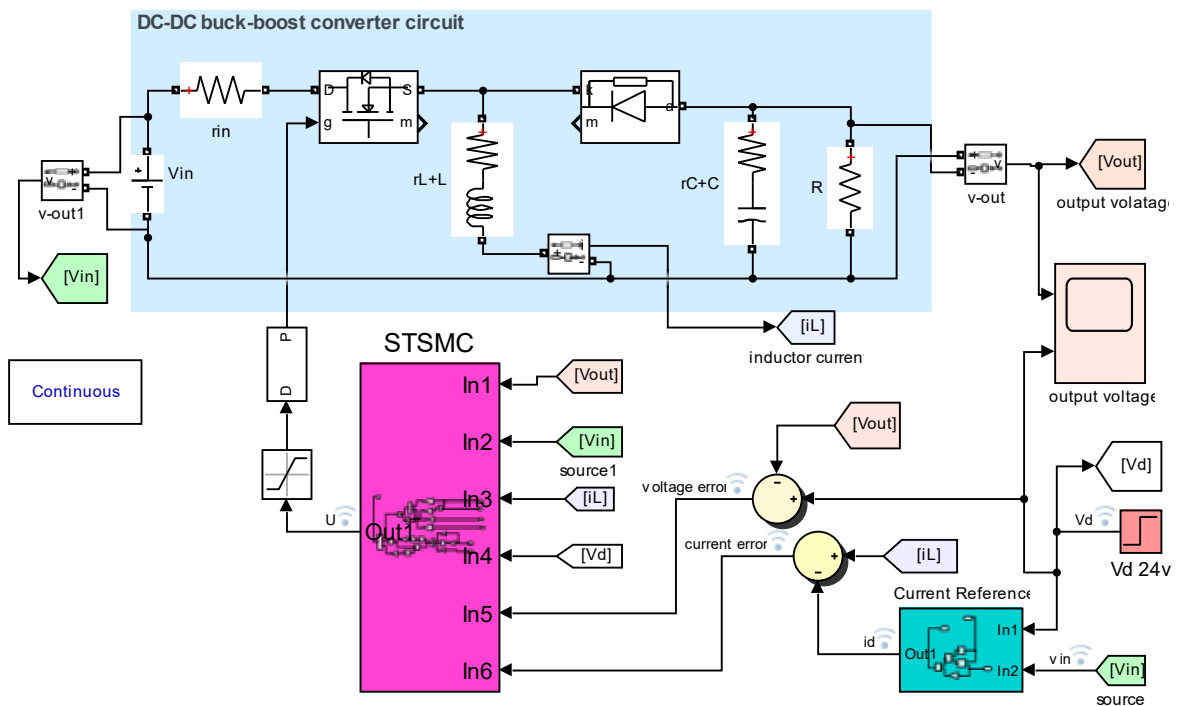


Figure 4.1 MATLAB/Simulink model of the proposed system

4.2 Simulation result

The proposed GA-PID, GA-STSMC, and PSO-STSMC controllers of the BBC system is validated and stabilized in this chapter using simulation tools. The simulation is done using the MATLAB/Simulink program.

4.2.1 System Open Loop Performance

The Simulink model depicted in Figure 4.1 is used to test and verify the open loop performance for the BBC. The settings used to run the simulation experiments are displayed in Table 4:1.

Table 4:1 System parameters for running the simulation

Descriptions	Parameters	Values	Units
Capacitance	C	16.93	μF
Capacitor ESR	C_r	50	$\text{m}\Omega$
Inductance	L	79.98	μH
Inductor Resistance	I_r	0.01	Ω
Switching Frequency	f_s	100	kHz
Maximum Load Resistance	$R_{L(\text{max})}$	14.4	Ω
Input Voltage	V_i	12	V
Desired Output Voltage	V_o	24	V

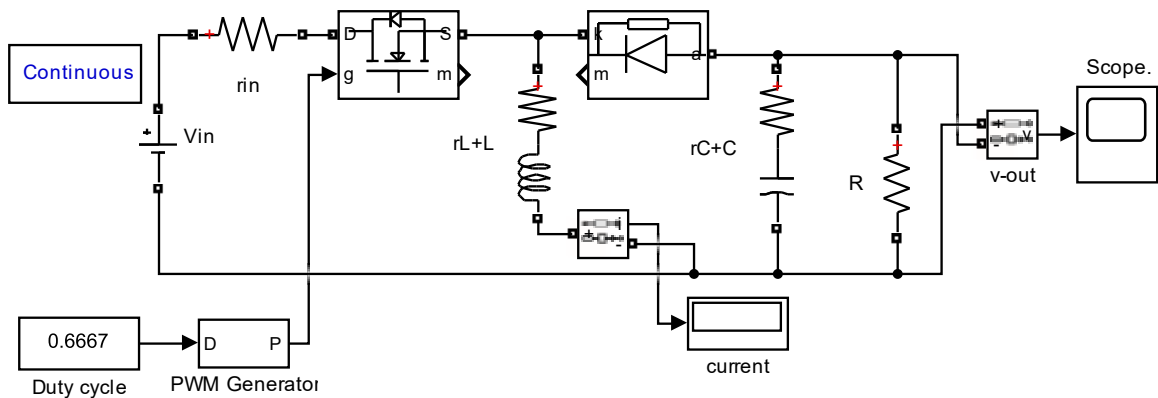


Figure 4.2 Simulink model of open loop BBC

It could be observed in Figure 4.3 and Figure 4.4 that the output voltage and inductor current response obtained using MATLAB/Simulink has a significant undesired overshoot that is

not required. In order to maximize system performance and provide quick and steady buck-boost converter performance, efficient controllers are required.

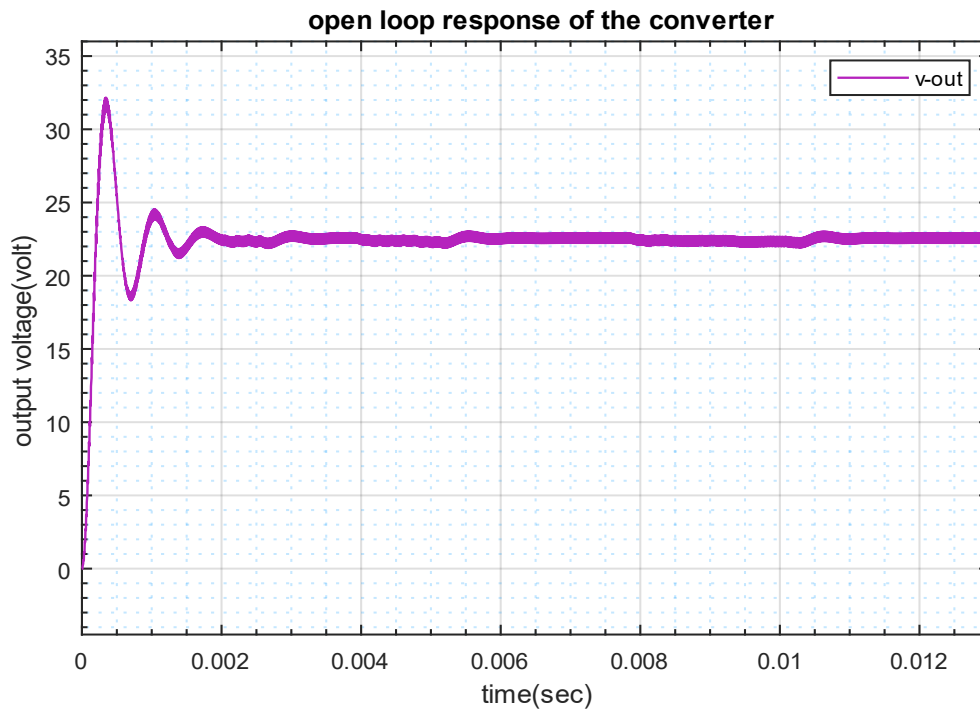


Figure 4.3 Open loop BBC's output voltage

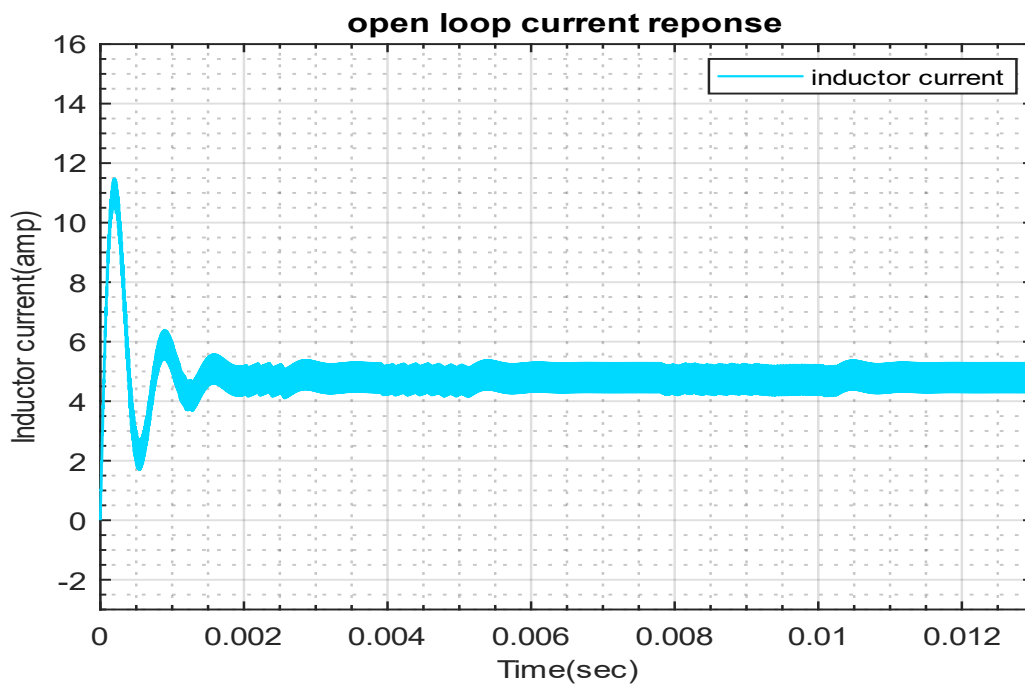


Figure 4.4 Open loop BBC's inductor current

4.2.2 System Performance with GA-PID

For the purpose of MATLAB/Simulink's performance demonstration of a DC-DC BBC by GA-PID controller, the converter's parameters are the same as that mentioned in Table 4.1 and using the tuned controller parameter that are listed in previous chapter.

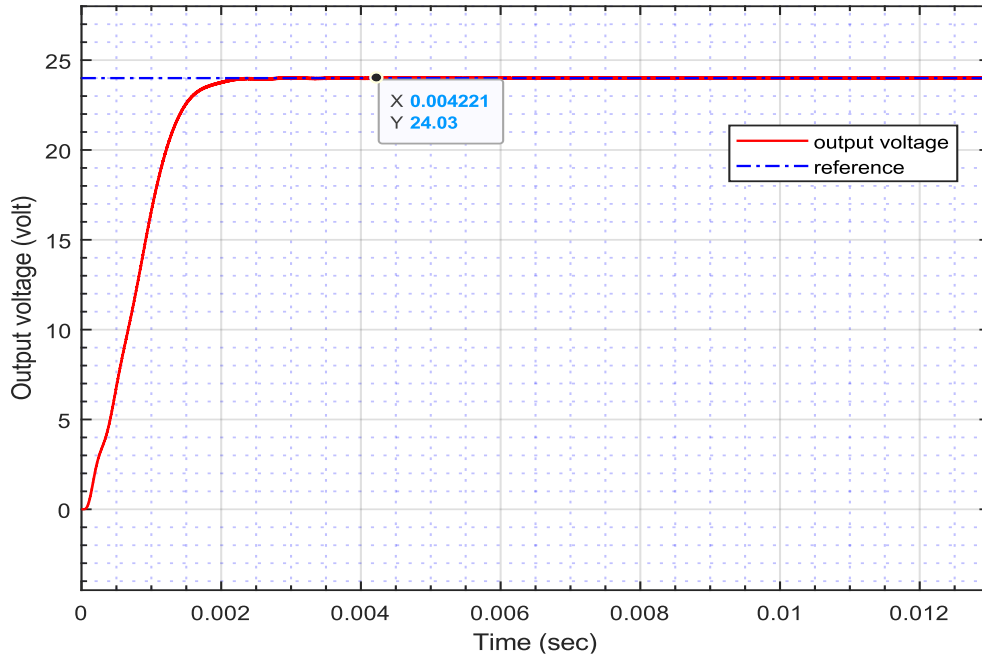
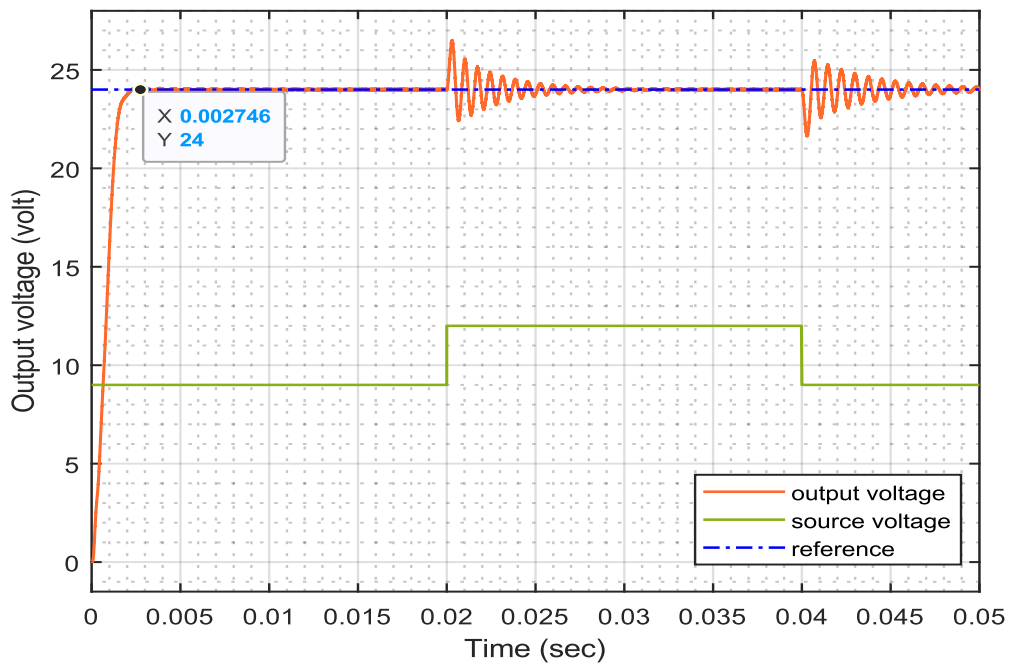


Figure 4.5 BBC's output voltage with GA-PID.

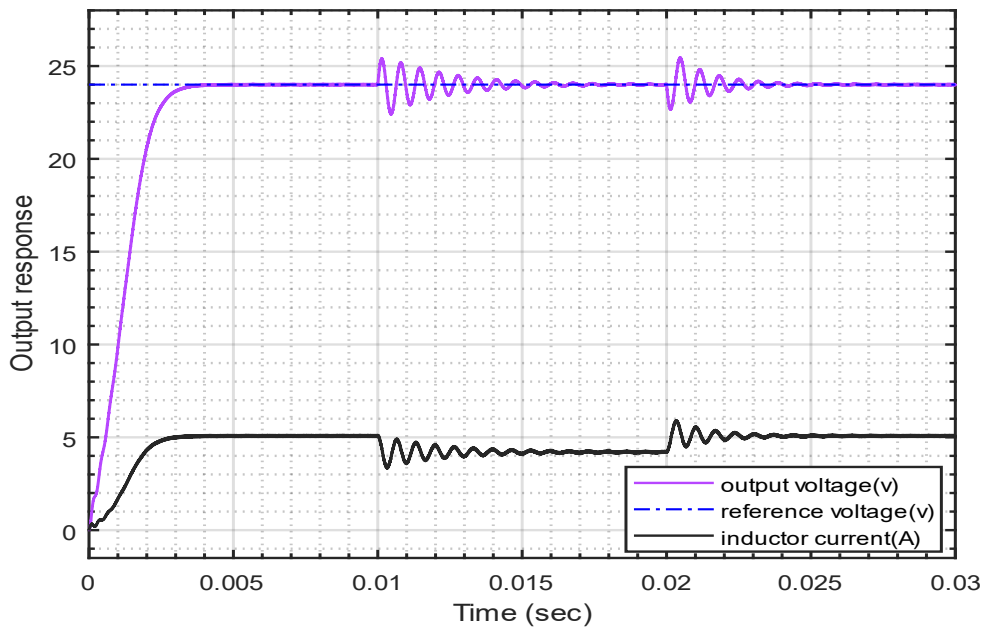
According to the outcome shown on Figure 4.5, the overshoot is significantly decreased when utilizing GA-PID for buck-boost converters. We can see that from nearly 0.001971 seconds until the conclusion of the evaluation period of 0.013 seconds, the actual output voltage follows the target output value.

4.2.3 System Performance with a GA-PID Controller in the Presence of Load Resistance and Input Voltage Disturbance

To evaluate the performance of the BBC by using GA-PID controller, two different input voltage changes were tested: firstly, from 9V to 12V, and then from 12V to 9V. Furthermore, the impact of load resistance variation was assessed by changing it from 14.4 Ω to 18 Ω , and then back to 14.4 Ω , while keeping the source voltage constant. The simulation result is depicted on Figure 4.6.



a) Input voltage vary from 9 to 12V and then to 9V



b) Load resistance vary from 14.4 to 18 Ω and then to 14.4 Ω

Figure 4.6 BBC's result with GA-PID in presence of input voltage and load resistance variation

As illustrated in Figure 4.6, the GA-PID created for the BBC records the required output voltage while taking into account load resistance and input voltage variation. This illustrates

that output voltage of the converter utilizing GA-PID is likely not affected by fluctuations in load resistance and that the controller automatically responds to input changes to maintain system stability and reject the effects of disturbance. The developed controller is reliable as should be needed.

4.2.4 System Performance with STSMC

The attributes of the converter correspond to the ones listed in Table 4.1, which illustrates the parameters of the system equipped with STSMC controller using MATLAB/Simulink. The result of the STSMC is depicted on Figure 4.7.

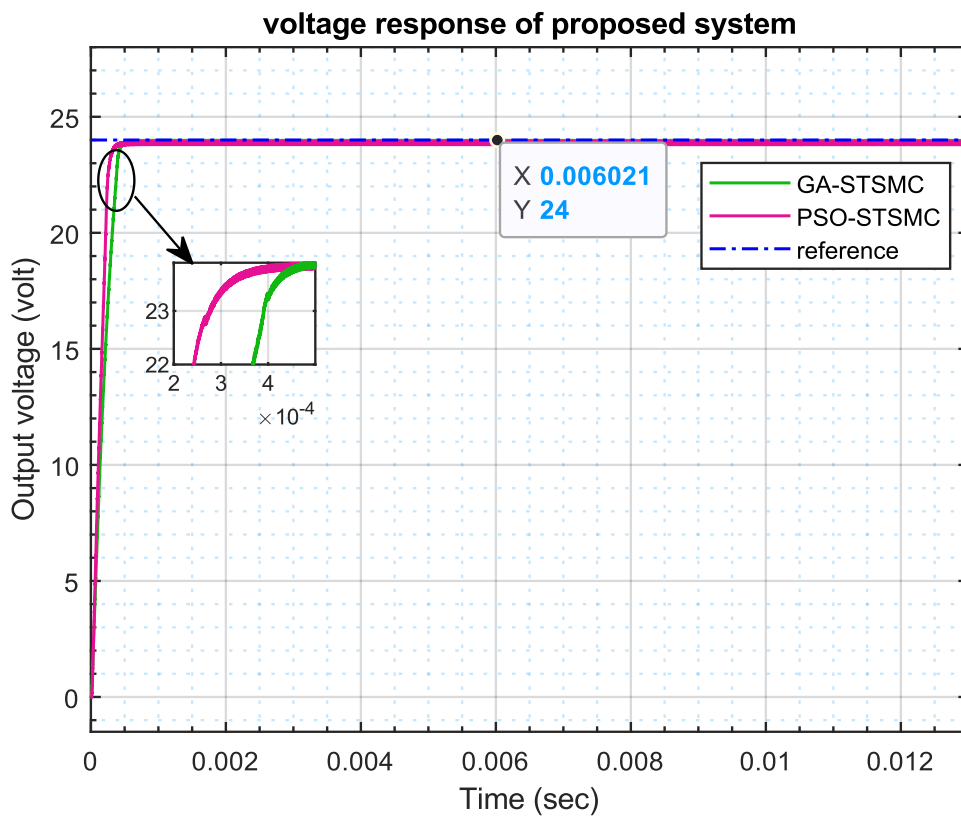


Figure 4.7 BBC's output voltage with STSMC

As depicted in Figure 4.7, it can be said that the proposed STSMC has better tracking performance for PSO optimization technique than GA and in turn much better than GA-PID controller.

4.2.5 System Performance with STSMC using staircase reference

The reference voltage (v_d) in this instance ranges from 15V \rightarrow 12V \rightarrow 24V \rightarrow 30V. The input voltage (V_g) is set at a constant 12V. Staircase reference voltage, and voltage of output is depicted in Figure 4.8 as a result of desired voltage (v_d) variation. Despite variations in reference voltage, the output voltage tracks the required voltage, as is evident from the figure.

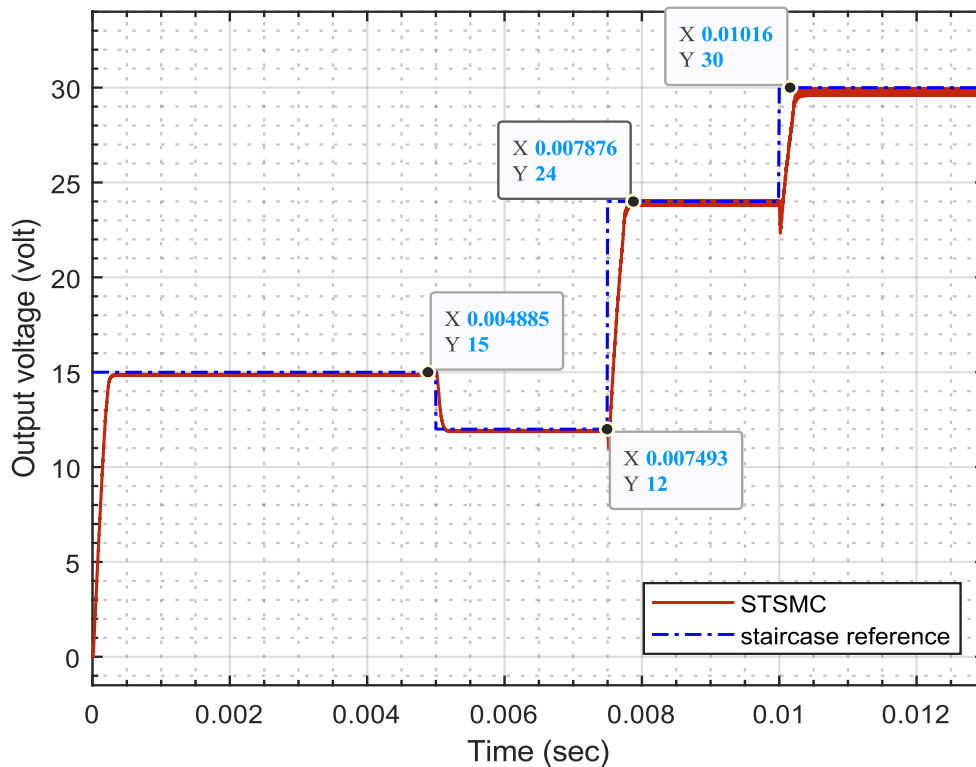
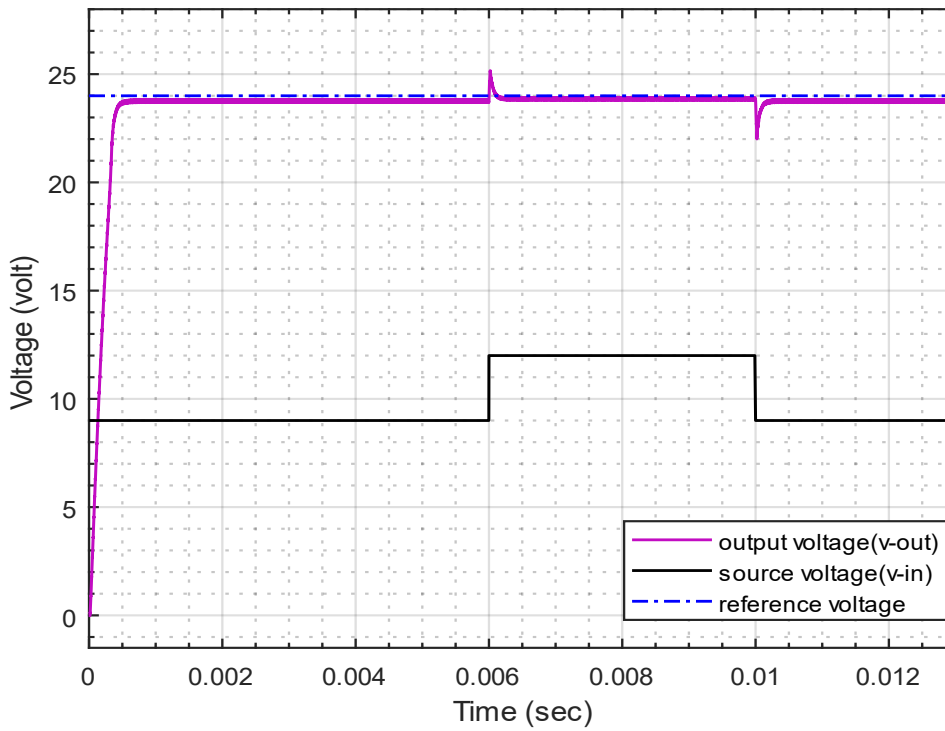


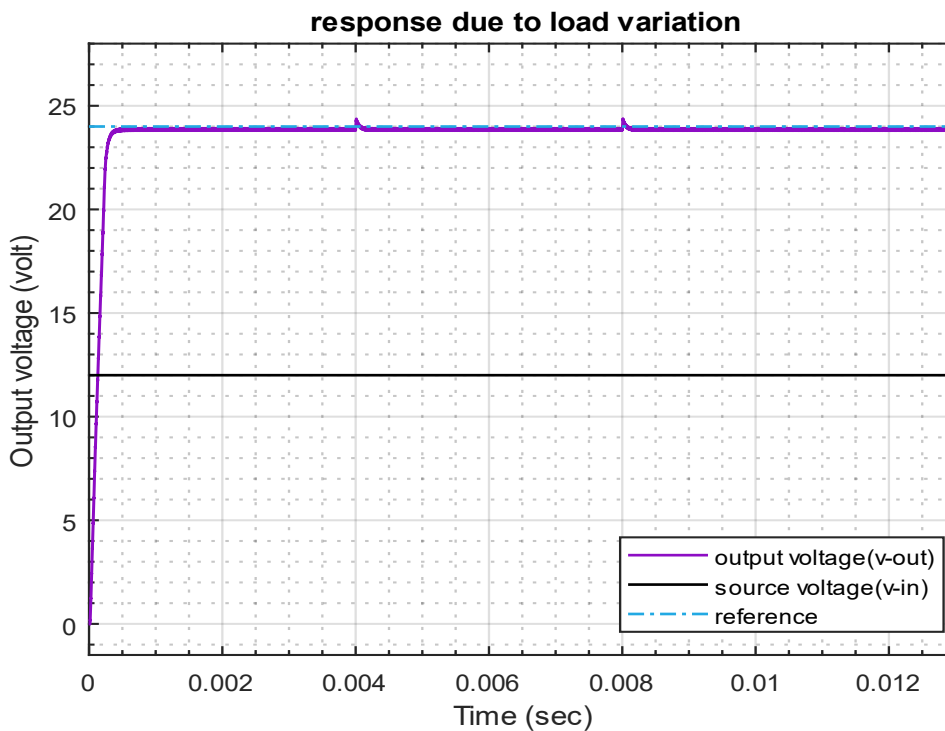
Figure 4.8 BBC's output voltage with STSMC using staircase reference

4.2.6 System Performance with STSMC Controller in presence of Disturbance in Load Resistance and Input Voltage

In order to evaluate the performance and robustness of the converter using GA-STSMC and PSO-STSMC controllers, the input voltage was varied from 9V to 12V and then from 12V to 9V. Furthermore, the load resistance was modified from 14.4 to 18 Ω and then back to 14.4 Ω while keeping the source voltage at 12V. These variations are carried out to analyse the effects of such changes. The simulation results can be observed in figure.



a) Input voltage vary from 9 to 12V and then to 9V



b) Load resistance vary from 14.4 to 18 Ω and then to 14.4 Ω

Figure 4.9 BBC's simulation result with STSMC for varying load resistance and input voltage

Figure 4.9 (a)-(b) findings indicate that the BBC utilizing a STSMC could handle variations in load resistance and input voltage. This indicates that the converter is capable of delivering the required output voltage regardless of variation in load resistance or input voltage. The STSMC controller, as illustrated in Figure 4.9, prevents significant input voltage changes from having an impact on the BBC's output voltage. Indicating that the necessary output voltage is attained for input voltage changes, it demonstrates that the BBC's actual output voltage overlaps the needed output value for variable input voltages.

4.2.7 System Performance Comparison for GA-PID, GA-STSMC and PSO-STSMC

As the BBC is needed to deliver the specified step output voltage (24v), Figure 4.10 displays the responses of the GA-PID controller, PSO-STSMC and GA-STSMC. It is obvious that compared to GA-STSMC and GA-PID control, PSO-STSMC control provides the desired output voltage more quickly. The rising and settling times of the left others' control strategies are longer than that of PSO-STSMC control, which has a comparatively short rising and settling time.

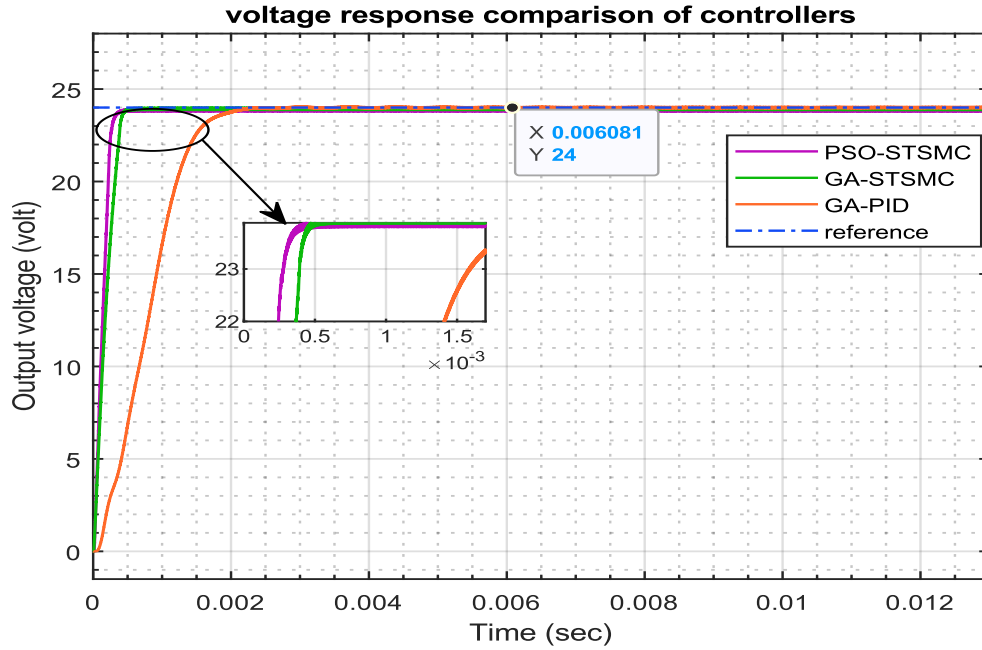


Figure 4.10 BBC's output voltage of GA-STSMC, PSO-STSMC and GA-PID

As seen in Figure 4.10, Based on the results of the simulation, it could be said that the PSO based STSMC controller performs slightly better than the GA based STSMC and much better than GA-PID controller and it is robust against disturbance and also the result is compare to the GA based fuzzy controller from the literature reviewed (Nugusa, 2021) as mentioned in Table 4:2.

4.2.8 System Performance Comparison of GA-PID, GA-STSMC and PSO-STSMC with staircase reference

The reference voltage (v_d) in this instance ranges from $15V \rightarrow 12V \rightarrow 24V \rightarrow 30V$. The input voltage (V_g) is kept at a constant 12V. Staircase reference voltage, and step output voltage (24v) is seen on Figure 4.11 as a result of reference voltage (v_d) variation.

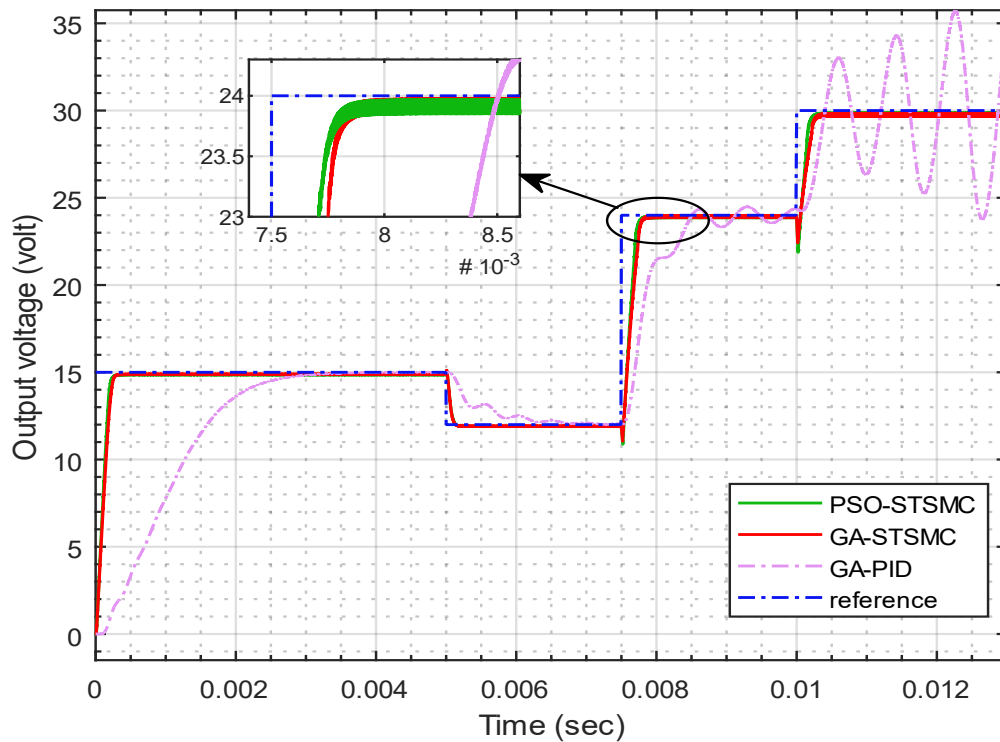


Figure 4.11 BBC's output voltage of GA-STSMC, PSO-STSMC and GA-PID with staircase reference

Despite variations in reference voltage, the output voltage tracks the reference voltage, as is evident from the figure but the GA-PID one is unable to sustain the variation in reference voltage so the proposed control methods have good disturbance rejection and variation. Generally, Table 4:2 lists the performance comparison of the controller with the desired voltage requirement.

Table 4:2 Comparisons of system performance measures

Controller	Performance measures		
	Rise time (msec)	Settling time (msec)	Overshoot/%
PSO-STSMC	0.19573	0.3108	0.1402
GA-STSMC	0.31471	0.4165	0.1757
GA-PID	1.101	1.802	0.412
GA-fuzzy	1.486	1.944	0.132

5 CONCLUSION AND RECOMMENDATION

5.1 Conclusion

This thesis introduced the use of STSMC in buck-boost Converter system. In this study, system modelling was carried out by averaging the converter's on- and off-state models to produce a single dynamic. Then, two separate control algorithms had been designed to control its dynamics. A PID controller and a super twisting sliding mode controller were the two control algorithms which are employed to verify the voltage control of the converter system.

The simulation was produced by MATLAB/Simulink to confirm the efficiency and performance of the proposed controller. PSO and GA were used to tune and optimize the controllers' gain.

The final set of results demonstrated that the system tracked the reference voltage with a very low tracking error. The proposed PSO-based STSMC, which has high system performance measure values of 0.19573 msec, 0.3108 msec, and 0.1402% of rise time, settling time, and maximum overshoot respectively, robustly tracks the given required reference environments in comparison to GA-based PID controller. The STSMC controller is unaffected by changes in input voltage and resistance. Finally, the result of the simulation shows that the buck-boost converter under the STSMC controller using PSO has better performance.

5.2 Recommendation

Examining the practical implementation of theoretical voltage regulation for buck-boost converter by using PSO and GA based STSMC, and PID controllers could be beneficial.

By undertaking nonlinear load analysis in order to explore the behaviour of the STSMC controller when the buck-boost converter is subjected to nonlinear loads. Additionally, investigating the controller's ability to handle load variations and nonlinear characteristics, such as varying power demands or non-linear impedance profiles, and assess its performance in maintaining stable voltage regulation under such conditions

On the other hand, implementing the STSMC controller on a hardware prototype of the buck boost converter and conduct experimental tests to validate its performance in real-world scenarios. Compare the experimental results with simulation results to assess the controller's practical applicability and verify its effectiveness under practical operating conditions.

It is recommended to explore methods such as parameter tuning algorithms, adaptive control strategies, or advanced optimization algorithms to enhance the controller's performance, achieve better transient response, and minimize control effort.

By addressing these recommendations, future work can further enhance the understanding, performance, and practical applicability of the STSMC controller for controlling voltage in buck-boost converters, leading to more efficient and reliable power conversion systems.

Acknowledgement

The research for this paper was financially supported by Adama Science and Technology University under the grant number of **ASTU/SM-R/720/23**, Adama, Ethiopia.

REFERENCES

- Abbasi, E., & Mahjoob, M. (2013). Controlling of Quadrotor UAV Using a Fuzzy System for Tuning the PID Gains in Hovering Mode. *10th International Conference on Advances in Computer Entertainment Technology*.
- Abderrezek, H., & Harmas, M. N. (2014). PSO Based Adaptive Terminal Sliding Mode Controllers for a DC-DC Converter. *International Journal of Computer Theory and Engineering*, 6(4), 302–306. <https://doi.org/10.7763/ijcte.2014.v6.879>
- Al-Mayyahi, A., Wang, W., & Birch, P. (2016). Design of Fractional-Order Controller for Trajectory Tracking Control of a Non-holonomic Autonomous Ground Vehicle. *Journal of Control, Automation and Electrical Systems*, 27(1). <https://doi.org/10.1007/s40313-015-0214-2>
- Al-Qaisi, M. A. F., Shehab, M. A., Al-Gizi, A., & Al-Saadi, M. (2019). High performance DC/DC buck converter using sliding mode controller. *International Journal of Power Electronics and Drive Systems*, 10(4). <https://doi.org/10.11591/ijpeds.v10.i4.pp1806-1814>
- Alam, W., Mehmood, A., Ali, K., Javaid, U., Alharbi, S., & Iqbal, J. (2018). Nonlinear control of a flexible joint robotic manipulator with experimental validation. *Journal of Mechanical Engineering*, 64(1). <https://doi.org/10.5545/sv-jme.2017.4786>
- Algamluoli, H. A. H. A. F. (2020). Voltage Controller of DC-DC Buck Boost Converter with Proposed PID Controller. *Int. J. Adv. Res. Comput. Eng. Technol*, 9, no, 1–4.
- Almawlawe, M. D., & Kovandzic, M. (2016). A Modified Method for Tuning PID Controller for Buck-Boost Converter. *International Journal of Advanced Engineering Research and Science*, 3(12). <https://doi.org/10.22161/ijaers/3.12.4>
- Clerc, M. (2010). Particle Swarm Optimization. *Part. Swarm Optim.*, No. doi: 10.1002/9780470612163.
- Conference, I. I. (2012). *2012 IEEE International Conference on Power Electronics, Drives and Energy System 2012 IEEE International Conference on Power Electronics, Drives and Energy Systems December 16-19, 2012, Bengaluru, Indias December 16-19, 2012, Bengaluru, India*.
- Dai, M., Qi, R., & Cheng, X. (2019). Super-twisting sliding mode control design for electric

- dynamic load simulator. *Chinese Control Conference, CCC, 2019-July*.
<https://doi.org/10.23919/ChiCC.2019.8865725>
- Farahmandrad, M., Ganjefar, S., Talebi, H. A., & Bayati, M. (2020). Design of higher-order sliding mode controller based on genetic algorithm for a cooperative robotic system. *International Journal of Dynamics and Control*, 8(1). <https://doi.org/10.1007/s40435-019-00516-x>
- G. V. Mohammed Dahleh, M. A. D. (n.d.). *Lectures on Dynamic Systems and Control*. .
- Gambhire, S. J., Kishore, D. R., Londhe, P. S., & Pawar, S. N. (2021). Review of sliding mode based control techniques for control system applications. In *International Journal of Dynamics and Control* (Vol. 9, Issue 1). <https://doi.org/10.1007/s40435-020-00638-7>
- Gaussian Fuzzy Logic Control*. (2012).
- Ghazali, R., Sam, Y. M., Rahmat, M. F., Hashim, A. W. I. M., & Zulfatman, . (2011). Performance Comparison between Sliding Mode Control with PID Sliding Surface and PID Controller for an Electro-hydraulic Positioning System. *International Journal on Advanced Science, Engineering and Information Technology*, 1(4). <https://doi.org/10.18517/ijaseit.1.4.91>
- Gitleman, L. (2014). NON LINEAR CONTROLLER FOR DC-DC BUCK CONVERTER. *Pap. Knowl. . Towar. a Media Hist, 1*, 1–19.
- Guldemir, H. (2011a). Modeling and Sliding Mode Control of DC-DC Buck-Boost Converter. *6th International Advanced Technologies Symposium (IATS'11), May*.
- Guldemir, H. (2011b). Study of Sliding Mode Control of DC-DC Buck Converter. *Energy and Power Engineering*, 03(04). <https://doi.org/10.4236/epe.2011.34051>
- Houssein, E. H., Gad, A. G., Hussain, K., & Suganthan, P. N. (2021). Major Advances in Particle Swarm Optimization: Theory, Analysis, and Application. *Swarm and Evolutionary Computation*, 63. <https://doi.org/10.1016/j.swevo.2021.100868>
- Hu, J., Zhang, Y., & Rakheja, S. (2022). Adaptive Trajectory Tracking for Car-Like Vehicles with Input Constraints. *IEEE Transactions on Industrial Electronics*, 69(3). <https://doi.org/10.1109/TIE.2021.3068672>
- Humaidi, A., & Hasan, A. (2019). Particle swarm optimization–based adaptive super-

- twisting sliding mode control design for 2-degree-of-freedom helicopter. *Measurement and Control*, 52, 002029401986686. <https://doi.org/10.1177/0020294019866863>
- Hussein, K. F., Abdel-Qader, I., & Hussain, M. K. (2015). Hybrid fuzzy PID controller for buck-boost converter in solar energy-battery systems. *IEEE International Conference on Electro Information Technology*, 2015-June, 70–75. <https://doi.org/10.1109/EIT.2015.7293323>
- L. Guo, V. Nelson, R. Nelms, J. Hung, S. M. (2006). *Design and Implementation of Digital Controllers for Buck and Boost Converters*.
- Lambora, A., Gupta, K., & Chopra, K. (2019). Genetic Algorithm- A Literature Review. *Proceedings of the International Conference on Machine Learning, Big Data, Cloud and Parallel Computing: Trends, Perspectives and Prospects, COMITCon 2019*. <https://doi.org/10.1109/COMITCon.2019.8862255>
- Lewis, F. L. (n.d.). *Dynamics and Control of Fixed-wing UAV Dynamics and Control of Fixed_wing UAV*.
- M. Theses and R. Citation. (2017). *ScholarWorks at WMU Voltage Controller for Simulating Transition between Boost – Buck -Boost Converter*.
- Mekonnen, C. (2019). DESIGN OF INTEGRAL SMC AND FUZZY PID CONTROLLER FOR VOLTAGE CONTROL OF A DC-DC BUCK-BOOST CONVERTER. *AASTU*. <https://nadre.ethernet.edu.et/record/4169/export/hx>
- Nasiri, M., Mobayen, S., & Zhu, Q. M. (2019). Super-Twisting Sliding Mode Control for Gearless PMSG-Based Wind Turbine. *Complexity*, 2019. <https://doi.org/10.1155/2019/6141607>
- Nugusa, D. (2021). Design of Genetic Algorithm Based Fuzzy Controller for Buck-Boost DC-DC Converters. *ASTU*. <http://213.55.101.20:8080/xmlui/handle/123456789/1789>
- Ouchen, S., Benbouzid, M., Blaabjerg, F., Betka, A., & Steinhart, H. (2021). Direct Power Control of Shunt Active Power Filter Using Space Vector Modulation Based on Supertwisting Sliding Mode Control. *IEEE Journal of Emerging and Selected Topics in Power Electronics*, 9(3). <https://doi.org/10.1109/JESTPE.2020.3007900>
- padhyay, S. B., Panda, P. G. K., Saha, P. P. K., & Das, P. S. (2015). Advance Control Techniques for DC/DC Buck Converter with Improved Performance. *International Journal of Advanced Research in Electrical, Electronics and Instrumentation*

Engineering, 04(01). <https://doi.org/10.15662/ijareeie.2015.0401029>

- R. Marouani, K. Echaieb, and A. M. (2012). *Converter in PV Grid-Connected System*. 281–284.
- Rahman, M. S. (2007). Buck converter design issues. In *Division of Electronic Devices Linkopings University*.
- S. Mirjalili, J. Song Dong, A. S. Sadiq, and H. F. (2020). Nature-inspired Optimizers. *Nature-Inspired Optimizers*, 811.
- Safari, N. (2012). Design of a DC/DC buck converter for ultra-low power applications in 65nm CMOS Process. *Thesis, March*.
- Shamim-Ul-Alam, M., Quamruzzaman, M., & Rahman, K. M. (2010). Fuzzy logic based sliding mode controlled DC-DC boost converter. *ICECE 2010 - 6th International Conference on Electrical and Computer Engineering, December*, 70–73. <https://doi.org/10.1109/ICELCE.2010.5700555>
- Shtessel, Y., Edwards, C., Fridman, L., & Levant, A. (2014). Sliding mode control and observation. In *Sliding Mode Control and Observation*. <https://doi.org/10.1007/978-0-8176-4893-0>
- Teja, S. V., Shanavas, T. N., & Patnaik, S. K. (2012). Modified PSO based sliding-mode controller parameters for Buck converter. *2012 IEEE Students' Conference on Electrical, Electronics and Computer Science: Innovation for Humanity, SCEECS 2012*, 3–6. <https://doi.org/10.1109/SCEECS.2012.6184759>
- Tolossa, Z. (2017). VOLTAGE CONTROL OF A DC-DC BUCK CONVERTER USING SECOND ORDER SLIDING MODE CONTROL. *AAU*. <http://etd.aau.edu.et/handle/123456789/4882>
- Utkin, V. I. (1992). Sliding Modes in Control and Optimization. In *Sliding Modes in Control and Optimization*. <https://doi.org/10.1007/978-3-642-84379-2>
- Verma, S. T. and G. (2018). “Simulation and Analysis of DC-DC Boost Converter Using Sliding Mode Controller under Variable Conditions. 13, 33–41. doi: %0A10.9790/1676-1301023341
- Wu, Y., Wang, L., Zhang, J., & Li, F. (2019). Path Following Control of Autonomous Ground Vehicle Based on Nonsingular Terminal Sliding Mode and Active Disturbance

Rejection Control. *IEEE Transactions on Vehicular Technology*, 68(7).
<https://doi.org/10.1109/TVT.2019.2916982>

Zhao, Y., Huang, P., & Zhang, F. (2018). Dynamic modeling and Super-Twisting Sliding Mode Control for Tethered Space Robot. *Acta Astronautica*, 143.
<https://doi.org/10.1016/j.actaastro.2017.11.025>

APPENDIXES

Appendix A: Specifications of the system Parameters

The parameters for the converter are derived from equations and subsequently adjusted to suit high switching frequency and low power applications. So, the MATLAB/Simulink implementation of the converter utilizes the following parameter values:

- $f=100$ kHz.
- $V_i= 12$ V.
- $V_d= 24$ V.
- $R= 14.4\Omega$.

Using the value listed above, we can get the duty cycle as:

$$D = \frac{V_o}{V_i} (1 - D) = 0.6667$$

The minimum inductor value is provided as,

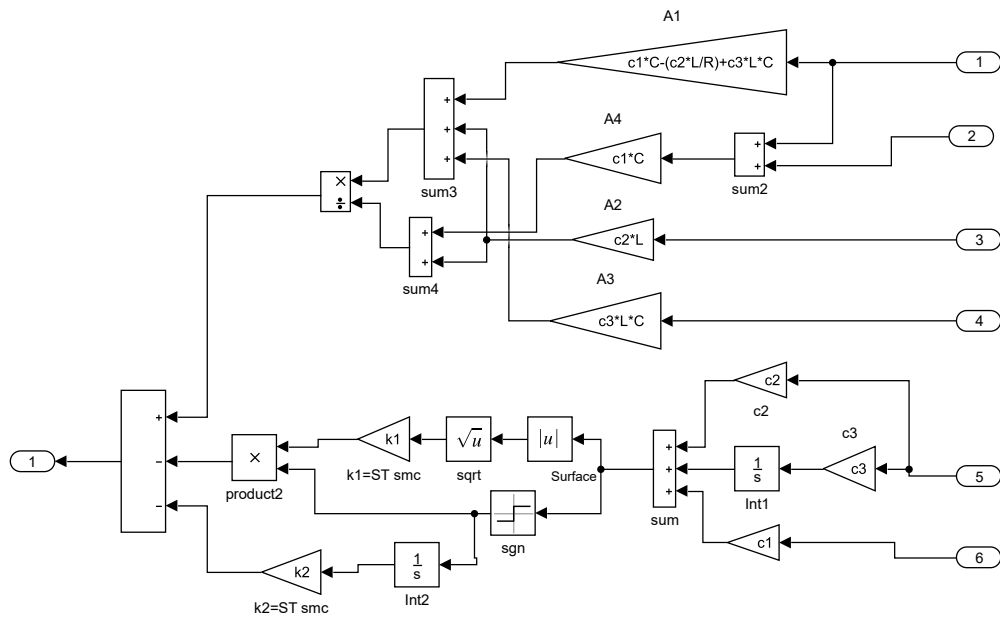
$$L_{\min} = \frac{(1-D)^2}{2f} R = 7.998\mu\text{H}$$

In order to address the continuous conduction, the inductor inductance value should be enough high by making it ten times the minimum value as $L=79.98 \mu\text{H}$.with capacitor ripple voltage of 0.4% (0.096v), the minimum capacitor value is provided as,

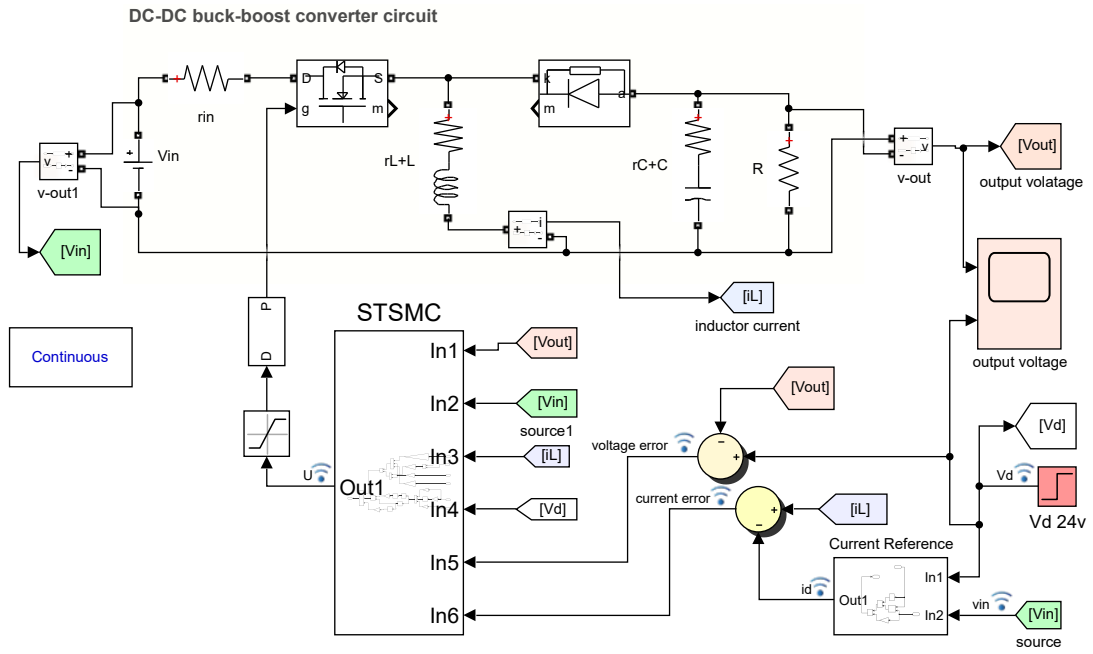
$$C_{\min} = \frac{(1-D)V_o}{8\Delta V_o L f^2} = 13.023\mu\text{F}$$

In order to decrease voltage's overshoot also ensure that the peak ripple voltage remains under a predetermined threshold, it is necessary for the capacitor value to exceed the minimum value. As a result, let's boost the capacitor's value by 30% of its minimum value, giving us $C=16.93 \mu\text{F}$.

Appendix B: Proposed STSMC Controller in Simulink



Appendix C: System Simulink Model



Appendix D: GA Code for Proposed STSMC

```
function GA_tune_simulinksmc
clear all
rng default
option = optimoption('ga', 'PlotFcn', @gaplotbestf);
option.Population_Size= 20;
option.Max_Generations= 20;
numvar= 5; % parameter's number
LB = [0.001 -20 -20 -10 -10]; % Lower bound
UB = [20 15 15 10 10]; % Upper bound
[xx , funval]= ga(@EvaluateObj, numvar, [],[],[],[], LB, UB, [], option)
function Obj= EvaluateObj(xx)
Simulink_Model= 'simulinksmc';
Load_system( Simulink_Model );
gain = getparams( Simulink_Model , 'model_workspace');
gain.assignin ('c1', xx(1));
gain.assignin ('c2', xx(2));
gain.assignin ('c3', xx(3));
gain.assignin ('k1', xx(4));
gain.assignin ('k2', xx(5));
Simoutt = sim(Simulink_Model, 'Save_Output', 'on');
% access time and error
tt= Simoutt.find(' t ');
ee= Simoutt.find(' e ');
k= length(tt);
abse= abs(ee); % absolute value of error
Obj= 0;
for j= 2:k
    step_size = tt(j) - tt(j-1);
    Obj = Obj + 0.5*step_size*(abse(j-1) + abse(j)); % Integral time of absolute value of error
end
```

Appendix E: PSO Code for Proposed STSMC

```
function PSO_tune_simulinksmc
clear all
rng default
option = optimoptions('particleswarm ');
option.PlotFcn= 'pswplotbestf';
option.MaxIterations= 30;
numvar= 5; % parameter's number to be tuned
LB= [0.001 -20 -20 -10 -10]; % Lower bound
UB= [20 15 15 10 10]; % Upper bound
[xx,funval]= particleswarm(@EvaluateObj,numvar, LB, UB, option)
function Obj= EvaluateObj(xx)
Simulink_Model= 'simulinksmc';
Load_system( Simulink_Model );
gain = getparams( Simulink_Model , 'model_workspace');
gain.assignin ('c1', xx(1));
gain.assignin ('c2', xx(2));
gain.assignin ('c3', xx(3));
gain.assignin ('k1', xx(4));
gain.assignin ('k2', xx(5));
Simoutt = sim(Simulink_Model, 'Save_Output', 'on');
% access time and error
tt= Simoutt.find(' t ');
ee= Simoutt.find(' e ');
k= length(tt);
abse= abs(ee); % absolute value of error
Obj= 0;
for j= 2:k
    step_size = tt(j) - tt(j-1);
    Obj = Obj + 0.5*step_size*(abse(j-1) + abse(j)); % Integral time of absolute value of error
end
```